Contemporary Mathematics
https://ojs.wiserpub.com/index.php/CM/

Research Article

The Endemic Trap: Proactive Early Intervention as the Key to Elimination in the Epidemiological Dynamics of Dual Thresholds

Moh Hasan*, **Faizal Rifky Fahreza**

Department of Mathematics, University of Jember, Jember, 68121, Indonesia
E-mail: hasan.fmipa@unej.ac.id

Received: 7 August 2025; **Revised:** 9 October 2025; **Accepted:** 15 October 2025

Abstract: Discrete system dynamics play a vital role in understanding the spread of infectious diseases, especially during pandemics. In this study, bifurcation analysis is employed on a discrete model incorporating interventions (vaccination and quarantine) and medical resource limitations to reveal qualitative changes in epidemic behavior. We investigate why early policy speed is crucial and how strategies must be adapted when a region faces an endemic state. Through the analysis of dual threshold bifurcation types I and II and numerical simulations, we demonstrate that, in the early phase (type I), complacency can lead to a serious dilemma, pushing the epidemic system (which describes how a disease moves through a population) into a costly, difficult-to-control endemic condition, and if a high endemic state is reached (type II) and medical capacity is exceeded, inadequate interventions risk causing an unsustainable return to high case numbers. Crucially, our analysis identifies this vulnerability as a false comfort zone: a fragile low-endemic state where minor disturbances can trigger a catastrophic return to high transmission. The ultimate threat is a dramatic surge in cases from shifts in transmission (e.g., new variants), which can undo all progress. These findings emphasize the importance of dynamic epidemiological thresholds and the need for proactive, consistent, and adaptive policies to mitigate future pandemic impacts.

Keywords: dual threshold bifurcation, epidemiological model, pandemic management, public health policy

MSC: 65L05, 34K06, 34K28

1. Introduction

Discrete dynamical systems are robust tools for understanding the complex behavior of epidemics. Consequently, numerous studies have used such systems to elucidate the fundamental dynamics of infectious disease spread. These highly versatile systems play a crucial role in modeling phenomena where evolution occurs in distinct, sequential steps. In a biological context, discrete dynamical systems are effective at predicting the development of and informing control strategies for disease vectors, e.g., mosquitoes [1]. In addition, these models can depict the dynamics of infectious disease transmission within a given population [2–4]. In-depth analysis of discrete dynamical systems is frequently dependent on various supporting theories, including bifurcation theory, to grasp how parameter changes can influence the dynamics of an epidemic.

DOI: https://doi.org/10.37256/cm.6620258182

In the context of dynamical systems, bifurcation refers to a qualitative change in the behavior of a system in response to small variations in a control parameter. This phenomenon has been a central focus of studies on discrete dynamical systems. Previous research has analyzed various bifurcations, including complex types such as period-doubling and Neimark-Sacker bifurcations [2, 5–8] as well as fundamental types such as transcritical, pitchfork, and saddle-node bifurcations [7, 9]. Furthermore, certain bifurcations can lead the system toward chaotic behavior, thereby indicating extreme complexity.

In the epidemiology field, studies on disease-spread dynamical systems have advanced rapidly since the development of the pioneering Kermack-McKendrick model. With the emergence of diverse disease characteristics and complex epidemic phenomena, these models have been expanded to analyze the effectiveness of various interventions, including vaccination, quarantine, and other control strategies [10–13]. In addition, these models are vital for predicting the achievement of herd immunity within a population [14, 15] and for assessing the impact of individual mobility on disease transmission [16]. Several studies have also integrated empirical data—e.g. hospitalization records, cumulative case counts, and diverse surveillance sources (including syndromic, environmental, genomic, serological, infoveillance, and mobility data)—to improve predictive accuracy and enable the exploration of more complex epidemic scenarios [17, 18].

Vaccination strategy modeling has evolved into a highly advanced research field. Numerous studies have developed complex frameworks to explore various key factors, such as the optimal interval between the first and second doses, the tradeoff between vaccination speed and dose spacing, and immune protection decline over time [19]. In these models, the population is typically divided into several groups (compartments) to reflect different protection levels: the first dose provides partial immunity, while the second dose boosts protection to be stronger and longer-lasting. Although detailed models with several compartments are considerably useful for forecasting and planning vaccine logistics, a simpler approach with only two dose compartments is considered in this study. This more concise structure allows for a deeper and clearer analysis of how vaccination, as a large-scale intervention, interacts with systemic constraints, such as limited medical resources. Using this approach, we can highlight the underlying nonlinear dynamics and bifurcation patterns, which are the main focus of this study.

Many previous studies have examined the impact of single interventions, such as vaccination or quarantine, and the presence of specific bifurcation types. However, there are still considerable gaps in understanding how these various interventions interact, particularly when combined with limited medical resources, creating a substantially more complex and vulnerable system dynamic. Few studies have examined bifurcation phenomena in epidemic models in detail—for instance, the existence of multiple endemic equilibria, where two stable states can coexist at the same parameter value [20], or codimension-two bifurcations, which signal deeper topological changes in system dynamics [21]. In particular, few studies analytically explain the emergence of several distinct bifurcation thresholds, which can determine the direction of system development. Consequently, the mechanisms that cause short-term policy successes to create long-term vulnerabilities remain poorly understood from a dynamical system perspective.

Fractional-order models have recently gained attention for their ability to capture memory effects in epidemic dynamics, and they are also valued for their flexibility in modifying mathematical frameworks to incorporate dynamical transmission, treatment, vaccination, and precautionary measures [22, 23]. Discrete models remain particularly relevant for epidemic analysis. They align more closely with the discrete nature of daily case data and are especially effective for investigating emerging bifurcations in the system. This study builds upon a discrete dynamical model first introduced in our previous study [24]. Although the previous study focused on the model's formulation and initial numerical simulations, the rich nonlinear dynamics inherent in the model, particularly the existence and policy implications of complex bifurcations, were unexplored. Therefore, the major novel contribution of the present study is to conduct a rigorous, in-depth bifurcation analysis of this model. In particular, we identify and mathematically characterize a "Dual Threshold Bifurcation"—a structure not discussed in the previous study. Notably, we link this complex mathematical phenomenon to a conceptual framework of "pandemic ironies" to provide a richer policy interpretation.

The recent global pandemic has highlighted the importance of understanding these dynamics. Policy decision-making must frequently deal with crucial dilemmas and significant uncertainty, and an inherent irony is observable in pandemic control efforts, where seemingly rational actions can result in unexpected consequences or lock the system into undesirable conditions [25, 26]. Such complexities arise from the nonlinear nature of disease spread, where minor parameter shifts can

trigger drastic changes in outcomes. This highlights the critical need for models that can capture these intricate behaviors and inform more robust strategies for navigating uncertainties.

In the early stages of a pandemic, aggressive interventions, e.g., strict mobility restrictions, massive increases in testing and tracing capacity, and rapid and comprehensive vaccination campaigns, are often considered crucial steps to fundamentally suppress the spread of the disease. Pandemic history shows that countries implementing decisive early measures tend to experience lower case burdens and quicker economic recovery. In contrast, delays or hesitant approaches can prolong the epidemic, overwhelm healthcare systems, and even cause such systems to become trapped in endemic conditions that are difficult to control. The experiences of several nations in adopting various early-phase interventions offer clear real-world examples of the potential consequences of these policy decisions [27, 28].

Through this methodological framework, by highlighting the critical importance of understanding system dynamics for effective navigation amidst uncertainty, this study attempts to investigate why health policies must be bold and swift, especially in the early phase of a pandemic. In addition, if a system becomes caught in an endemic trap, this study analyzes how intervention strategies should adapt to steer the system toward a more controlled state and what the risks are if such adaptation fails. Here, emphasis is placed on the endemic trap concept and the identification of how, over time, unintended policy consequences can influence the evolution of a pandemic. The remainder of this paper is structured as follows. Section 2 presents the formulation of the discrete epidemic model, which incorporates vaccination, quarantine, and medical resource limitations. Section 3 provides a detailed analysis of the model, including its equilibrium points, stability, and complex bifurcations, followed by an in-depth discussion of their policy implications. Finally, Section 4 concludes this study with a summary of the key findings and their relevance for future pandemic preparedness.

2. Methods

In this study, an analytical and numerical approach is employed to investigate the dynamics of infectious disease spread with a specific focus on policy implications. This base model is selected because it provides a comprehensive analysis framework. It already integrates several critical, interacting interventions: a two-dose vaccination scheme, quarantine protocols, and a nonlinear recovery function dependent on medical resource capacity. Although this model can be formulated in continuous form (differential equations), we select a discrete-time approach (difference equations) for two main reasons. First, epidemiological data, such as daily cases and vaccinations, are typically reported daily, making discrete models more suitable. Second, discrete systems can exhibit richer dynamics, including period-doubling bifurcations and routes to chaos, which rarely appear in continuous models. Because our focus is on understanding the nonlinear dynamics and critical transitions relevant to policy, a discrete framework offers a more appropriate foundation for this analysis. We employ a discrete epidemic model adapted from Fahreza et al. [24], which focuses on the model's formulation and initial validation. The novel analytical contribution of this study lies in the detailed bifurcation analysis of the model and subsequent interpretation of its complex dynamics, which are presented in the Results and Discussion section. The dynamics of the system are described by the following equations:

$$S_{t+1} = S_t + \Lambda - \lambda S_t I_t - \lambda q S_t Q_t - \varphi_1 S_t + \rho R_t - \mu S_t,$$

$$V_{1_{t+1}} = V_{1_t} + \varphi_1 S_t - \lambda p V_{1_t} I_t - \lambda pq V_{1_t} Q_t - \varphi_2 V_{1_t} - \mu V_{1_t},$$

$$V_{2_{t+1}} = V_{2_t} + \varphi_2 V_{1_t} - \lambda r V_{2_t} I_t - \lambda rq V_{2_t} Q_t - \mu V_{2_t},$$

$$I_{t+1} = I_t + \lambda S_t I_t + \lambda p V_{1_t} I_t + \lambda r V_{2_t} I_t + \lambda q S_t Q_t + \lambda pq V_{1_t} Q_t + \lambda rq V_{2_t} Q_t - \tau_1 I_t + \tau_2 Q_t - \mu I_t - \zeta I_t - f(I_t),$$

$$
\begin{aligned}
Q_{t+1} &= Q_t + \tau_1 I_t - \tau_2 Q_t - \gamma_n Q_t - \zeta d Q_t - \mu Q_t, \\
R_{t+1} &= R_t + \gamma_n Q_t - \rho R_t - \mu R_t + f(I_t), \\
D_{t+1} &= D_t + \zeta I_t + \zeta d Q_t.
\end{aligned} \tag{1}
$$

The function $f(I_t)$, which represents the recovery rate dependent on medical capacity, is defined as follows.

$$
f(I_t) = \begin{cases} (\gamma_n + \gamma_m) I_t, & I_t \leq I_b \\ (\gamma_n + \gamma_m) I_b + \gamma_n (I_t - I_b), & I_t > I_b. \end{cases}
$$

This model divides the population into seven compartments. S_t denotes the susceptible population, and V_{1_t} and V_{2_t} denote the first- and second-dose vaccinated populations, respectively. The infected population is split into two groups: I_t for moderately to severely infected individuals requiring medical intervention and Q_t for mildly infected individuals in self-quarantine. Moreover, R_t is the recovered population, and D_t is the cumulative number of deceased individuals. A full description of each parameter of the model is shown in Table 1. The subscript t denotes the time step. Furthermore, I_b represents the medical resource threshold, defined as the maximum number of infected individuals that the healthcare system can treat with full effectiveness via normal and medically assisted recovery.

Table 1. Parameters of System (1)

Parameter	Description	Parameter	Description
λ	Infection rate	ρ	Reinfection rate
φ_1	First-dose vaccination rate	p	Reduction in infection rate due to first-dose vaccination
φ_2	Second-dose vaccination rate	r	Reduction in infection rate due to second-dose vaccination
τ_1	Transfer rate from $I(t)$ to $Q(t)$	q	Reduction in infection rate due to quarantine
γ_n	Normal recovery rate	d	Reduction in mortality rate due to vaccine
ζ	Covid-19 mortality rate	Λ	Normal birth rate
τ_2	Transfer rate from $Q(t)$ to $I(t)$	μ	Normal mortality rate
γ_m	Medically assisted recovery rate		

The proposed model mathematically represents key public health interventions as follows. First, vaccination is modeled as a two-dose strategy. The parameter φ_1 represents the rate at which susceptible individuals (S_t) receive their first vaccine dose, moving them to the V_{1_t} compartment. Subsequently, φ_2 is the rate of second-dose administration, transitioning individuals to the fully vaccinated V_{2_t} compartment. The vaccine's efficacy is captured by parameters p and r (where $0 < r < p < 1$), which reduce but do not eliminate the infection risk. For instance, the term $\lambda p V_{1_t} I_t$ indicates that first-dose vaccinated individuals have a reduced probability of infection compared with unvaccinated individuals. Second,

quarantine is modeled as a mechanism to reduce transmission from infected individuals. The parameter τ_1 governs the rate at which individuals from the infected class (I_t) move into the quarantined class (Q_t). The effectiveness of this isolation is represented by the parameter q (where $0 \leq q < 1$), which reduces the transmission rate from the quarantined population. A value of $q = 0$ indicates a perfect quarantine where individuals in Q_t are completely isolated and cannot spread the disease, whereas a value close to 1 indicates less effective quarantine.

In this study bifurcation analysis allows us to identify critical control parameter values where qualitative changes in system behavior occur, e.g., the emergence or disappearance of equilibrium points, or changes in their stability. Specifically, we focus on an in-depth elaboration of the dual threshold bifurcation that arises in the system. This enables us to systematically explain the model's nonlinear complexities and their implications for policy responses. In addition, numerical simulations are performed to elucidate the analytical findings and investigate the system dynamics under various intervention scenarios, particularly in the context of hysteresis and endemic traps. The results are then discussed in the context of real-world observations from the COVID-19 pandemic globally, using illustrative case studies from various countries to demonstrate the model's policy relevance.

3. Results and discussion

3.1 *Equilibrium point and stability analysis*

For the model to be epidemiologically meaningful, we must ensure that all state variables remain non-negative and that the total population is bounded for all time $t \geq 0$. The detailed proofs for the positivity and boundedness of the solutions to System (1) are presented in Appendix A.

3.1.1 *Disease-Free Equilibrium (DFE)*

The DFE point of System (1), denoted $\Omega_0 = \left(S_0, V_{1_0}, V_{2_0}, 0, 0, 0, 0\right)$, represents a state in which the disease is absent from the system ($I = Q = R = D = 0$). By setting $X_{t+1} = X_t = X^*$ for all compartments, signifying that the population in each compartment remains constant over time, and then substituting $I^* = Q^* = R^* = D^* = 0$, the nonzero compartments of the DFE are derived as follows:

$$S_0 = \frac{\Lambda}{k_1}, \quad V_{1_0} = \frac{\Lambda\varphi_1}{k_1 k_2}, \quad V_{2_0} = \frac{\Lambda\varphi_1\varphi_2}{\mu k_1 k_2},$$

where $k_1 = \mu + \varphi_1$ and $k_2 = \mu + \varphi_2$. Here, it is evident that an increase in the first-dose vaccination rate (φ_1) reduces the susceptible population (S_0), and an increase in the second-dose vaccination rate (φ_2) increases the fully vaccinated population (V_{2_0}). This reflects the expected dynamic where vaccination effectively reduces the pool of susceptible individuals.

Then, the basic reproduction number ($\mathscr{R}_0$) of System (1) is determined using the next-generation matrix approach $\left(\mathbf{K} = \mathbf{F}\left[\mathbf{I} - \mathbf{T}\right]^{-1}\right)$ [29–31], with a focus on the infected population compartments I_t and Q_t. Epidemiologically, $\mathscr{R}_0$ represents the average number of new cases caused by a single infected individual in a fully susceptible population, where no one has been vaccinated or developed immunity. Here, the matrices $\mathbf{F}$ and $\mathbf{T}$ represent the new infections and the transitions between infected states, respectively. The matrices $\mathbf{F}$ and $\mathbf{T}$ for System (1) are obtained as follows:

$$\mathbf{F}(\Omega_0) = \begin{bmatrix} \frac{\Lambda\lambda((p\varphi_1+k_2)\mu+\varphi_1\varphi_2 r)}{\mu k_1 k_2} & \frac{\Lambda\lambda q((p\varphi_1+k_2)\mu+\varphi_1\varphi_2 r)}{\mu k_1 k_2} \\ 0 & 0 \end{bmatrix},$$

$$\mathbf{T}(\Omega_0) = \begin{bmatrix} -k_3+1 & \tau_2 \\ \tau_1 & -k_4+1 \end{bmatrix},$$

where $k_3 = \tau_1 + \mu + \zeta + \gamma_n + \gamma_m$ and $k_4 = \tau_2 + \gamma_n + \zeta d + \mu$. Here, k_3 denotes the total rate of individuals leaving the population compartment I_t (due to quarantine, natural death, disease-induced death, and recovery), and k_4 denotes the total rate of individuals leaving the population compartment Q_t.

Thus, the next-generation matrix $\mathbf{K} = \mathbf{F}\left[\mathbf{I} - \mathbf{T}\right]^{-1}$ is derived as follows.

$$\mathbf{K} = \begin{bmatrix} \frac{\Lambda\lambda((p\varphi_1+k_2)\mu+\varphi_1\varphi_2 r)(q\tau_1+k_4)}{\mu k_1 k_2(k_3k_4-\tau_1\tau_2)} & \frac{\Lambda\lambda((p\varphi_1+k_2)\mu+\varphi_1\varphi_2 r)(qk_3+\tau_2)}{\mu k_1 k_2(k_3k_4-\tau_1\tau_2)} \\ 0 & 0 \end{bmatrix}.$$

The basic reproduction number $\mathscr{R}_0$ is the spectral radius of matrix $\mathbf{K}$, which is obtained as follows:

$$\mathscr{R}_0 = \frac{\Lambda\lambda((p\varphi_1 + k_2)\mu + \varphi_1\varphi_2 r)(q\tau_1 + k_4)}{\mu k_1 k_2(k_3k_4 - \tau_1\tau_2)}. \tag{2}$$

In addition, based on Theorem 4.4 in the literature [30], the following corollary is obtained regarding the stability of Ω_0.

Corollary 1 The DFE Ω_0 of System (1) is locally asymptotically stable if $\mathscr{R}_0 < 1$ and unstable if $\mathscr{R}_0 > 1$, where $\mathscr{R}_0$ is obtained using Equation (2).

The detailed proof of this corollary, based on the Jury stability criteria, is presented in Appendix B.

The derived basic reproduction number $\mathscr{R}_0$ provides crucial insights into the factors that influence the spread of a disease. It reveals a proportional relationship with the infection rate λ, indicating that higher transmission rates lead to greater spread potential. Conversely, the vaccine efficacy parameters (i.e., p and r) and the quarantine effectiveness factor q exhibit an inverse relationship with $\mathscr{R}_0$, demonstrating that enhanced vaccination coverage and more effective quarantine measures reduce the disease's spread potential. This analysis shows that the epidemic will disappear if $\mathscr{R}_0 < 1$. However, the crucial next question is what happens if the epidemic does not disappear? To answer this, we must analyze the conditions under which a disease persists in a population, i.e., the existence of an Endemic Equilibrium (EE) point.

3.1.2 *EE point*

The EE point of System (1) is analyzed to understand the behavior of the system when the disease persists within the population, indicated by $I > 0$ (and consequently positive values for Q, R, and D). The existence of an EE is significantly influenced by the availability of medical resources, giving rise to two primary scenarios based on the infected population size I_t relative to the medical resource threshold I_b. Thus, two types of EE points are defined, i.e., Ω_1 for $I_t \leq I_b$, and Ω_2 for $I_t > I_b$.

Case 1: EE when $I^* \leq I_b$

When the infected population is at or below the medical resource threshold (i.e., $I_t \leq I_b$), the recovery function is given as $f(I_t) = (\gamma_n + \gamma_m) I_t$. Here, the nonzero equilibrium components $S_1, V_{1_1}, V_{2_1}, I_1, Q_1$, and R_1 are derived by setting the system to equilibrium $(X_{t+1} = X_t = X^*)$ and solving the resulting system of equations. Then, these equilibrium values can be substituted into the definition of the force of infection, i.e., $\alpha = \lambda\left(I_1 + qQ_1\right)$, to express α in terms of the system

parameters (detailed expressions for these components are provided in Appendix C). The parameter α indicates the rate at which susceptible individuals contract the disease within the population.

By substituting all the aforementioned components, we can summarize the entire system dynamics into a single key equation that links the rate of infection (α) with $\mathscr{R}_0$. This equation is in the form of a cubic polynomial, whose solutions determine whether endemic conditions exist:

$$A\alpha^3 + B\alpha^2 + C\alpha + E\,(1-\mathscr{R}_0) = 0, \tag{3}$$

where A, B, C, and E are coefficients (detailed expressions are given in Appendix D). Notably, coefficients A and E are definitively negative.

The endemic equilibria of the system are represented by the positive real solutions of this cubic equation. Note that Equation (3) can yield up to three positive real solutions, indicating the possibility of multiple endemic states, and the values of the coefficients A, B, C, and E are examined to analyze the existence of these points. Given that coefficient A and E are definitely negative, the analysis primarily focuses on coefficients B and C. Further insights into the existence of an EE can be gained by analyzing the extremum values of Equation (3), which occur when the first derivative of the equation equals zero.

$$3A\alpha^2 + 2B\alpha + C = 0. \tag{4}$$

The solutions for α at the extremum points are given by $\frac{-B\pm\sqrt{B^2-3AC}}{3A}$. The existence of these extremum points requires the discriminant B^2-3AC to be positive. From the form of Equation (3), the function $\mathscr{R}_0$ can be defined as $\mathscr{R}_0 = h(\alpha) = \frac{A\alpha^3+B\alpha^2+C\alpha+E}{E}$, and the following proposition is formulated regarding the existence of the system's EE by analyzing the values of coefficients B, C, the discriminant B^2-3AC, and the value of $\mathscr{R}_0$.

Proposition 1 System (1) has

i) one EE if $\mathscr{R}_0 > 1$,

ii) two endemic equilibria if $h\left(\frac{-B-\sqrt{B^2-3AC}}{3A}\right) < \mathscr{R}_0 \leq 1$ and $C > 0$,

iii) two endemic equilibria if $h\left(\frac{-B-\sqrt{B^2-3AC}}{3A}\right) < \mathscr{R}_0 < 1$, $B^2-3AC > 0$, $B > 0$, and $C < 0$,

iv) three endemic equilibria if $1 \leq \mathscr{R}_0 < h\left(\frac{-B+\sqrt{B^2-3AC}}{3A}\right)$, $B^2-3AC > 0$, $B > 0$, and $C < 0$.

No EE exists in the system beyond the previously identified parameter conditions.

In summary, Proposition 1 states that the dynamics of an epidemic are not as simple as "disappear or spread". Depending on the complex interaction between parameters, such as vaccine efficacy and quarantine rate (mathematically summarized in coefficients B and C), the system can have up to three endemic conditions. Scenarios (ii), (iii), and (iv) are the most interesting from a policy perspective because they show that outbreaks can persist (two equilibria) or even have some degree of severity (three equilibria) even when $\mathscr{R}_0$ approaches or is below 1.

Case 2: EE when $I^* > I_b$

Following the analysis for $I_t \leq I_b$, the EE when the infected population exceeds the medical resource threshold (i.e., $I_t > I_b$) is analyzed. This condition, representing an overwhelmed healthcare system, triggers significant changes in the epidemic dynamics due to the modified recovery function $f(I_t) = (\gamma_n+\gamma_m)I_b + \gamma_n(I_t - I_b)$. Here, to facilitate a more direct understanding of this transition and the system's behavior under resource limitation conditions, the analysis shifts focus from $\mathscr{R}_0$ and α to the relationship between the number of infected individuals I and the infection rate λ.

For this case, the EE is defined as $\Omega_2 = (S_2, V_{1_2}, V_{2_2}, I_2, Q_2, R_2, D_2)$, and the nonzero equilibrium components S_2, V_{1_2}, V_{2_2}, Q_2, and R_2 can be expressed in terms of I_2 and λ (detailed expressions are given in Appendix E). Substituting

these equilibrium components into the governing equation for I_2 results in a quartic equation describing how I_2 changes with variations in λ:

$$h_1(I_2) = A_1 I_2^4 + B_1 I_2^3 + C_1 I_2^2 + E_1 I_2 + F_1 = 0, \tag{5}$$

where

$$A_1 = \lambda^3 A_2, \qquad B_1 = (q\tau_1 + k_4)^2 \lambda^2 (\lambda B_2 + B_3),$$

$$C_1 = (q\tau_1 + k_4) k_4^2 \lambda (\lambda C_2 + C_3), \qquad E_1 = k_4^3 (\lambda E_2 + E_3).$$

The parameters A_2, B_2, B_3, C_2, C_3, E_2, E_3, and F_1 are detailed in Appendix F. The positive real solutions of this quartic equation represent the system's EE when $I_t > I_b$.

3.2 *Bifurcation existence analysis*

This section analyzes the system's bifurcations, which represent critical shifts in behavior caused by changes in specific parameter values. From an epidemiological perspective, this indicates a critical point where small changes in parameters (e.g., transmission rate or vaccination coverage) can drastically alter the system's behavior, e.g., from a controlled outbreak to a surge in cases. Understanding these bifurcations is crucial for understanding the complex dynamics of a pandemic.

3.2.1 *Saddle-node bifurcation and multiple endemic equilibria*

A saddle-node bifurcation is a phenomenon where two equilibrium points (typically one stable and one unstable) emerge or annihilate each other. Epidemiologically, this saddle-node bifurcation explains how a high-level endemic condition can suddenly appear or disappear. This is the mathematical mechanism behind the sudden surge of an outbreak from seemingly controllable levels to unmanageable levels. Proposition 1 shows that our system can exhibit up to two EEs when $\mathscr{R}_0 < 1$, which occurs when the extremum values in Equation (3) are positive, a condition that strongly suggests a saddle-node bifurcation.

To confirm this, we analyzed the stability of Equation (3) at its extremum points. A saddle-node bifurcation occurs when the first derivative of Equation (3), given by $g(\alpha) = 3A\alpha^2 + B\alpha + C$ (Equation (4)), equals zero at these points. Proposition 1 identifies two primary conditions for the existence of two EEs, both of which lead to $g(\alpha) = 0$ at their respective extremum points:

i) when $\mathscr{R}_0 < 1$ and $C > 0$, the positive extremum point $\frac{-B-\sqrt{B^2-3AC}}{3A}$ yields $g\left(\frac{-B-\sqrt{B^2-3AC}}{3A}\right) = 0$,

ii) when $\mathscr{R}_0 < 1$, $B > 0$, $B^2 - 3AC > 0$, and $C < 0$, the two extremum points $\frac{-B\pm\sqrt{B^2-3AC}}{3A}$ both result in $g\left(\frac{-B\pm\sqrt{B^2-3AC}}{3A}\right) = 0$.

These findings confirm that parameter changes satisfying these conditions trigger a saddle-node bifurcation, thereby causing significant shifts in the epidemic's dynamics. This leads to the following proposition.

Proposition 2 The EE of System (1) undergoes a saddle-node bifurcation at:

i) $\mathscr{R}_0 = h\left(\frac{-B-\sqrt{B^2-3AC}}{3A}\right)$ if $C > 0$,

ii) $\mathscr{R}_0 = h\left(\frac{-B\pm\sqrt{B^2-3AC}}{3A}\right)$ if $B^2 - 3AC > 0$, $B > 0$, and $C < 0$.

3.2.2 *Transcritical Bifurcation at $\mathscr{R}_0 = 1$*

A crucial shift in the stability of the system occurs when $\mathscr{R}_0 = 1$, which indicates a transcritical bifurcation. At this point, the DFE transitions from stable to unstable, and an EE emerges as $\mathscr{R}_0$ exceeds 1. To demonstrate this, we compute the Jacobian matrix of the discrete system at the DFE, $\Omega_0 = (\frac{k_2\mu(k_3k_4-\tau_1\tau_2)}{K}\mathscr{R}_0,\ \frac{\varphi_1\mu(k_3k_4-\tau_1\tau_2)}{K}\mathscr{R}_0,\ \frac{\varphi_1\varphi_2(k_3k_4-\tau_1\tau_2)}{K}\mathscr{R}_0,\ 0,\ 0,\ 0,\ 0)$, where $K = ((p\varphi_1+k_2)\mu+\varphi_1\varphi_2 r)\lambda(\tau_1 q+k_4)$. Here, a transcritical bifurcation is confirmed if one of the Jacobian's eigenvalues equals 1.

Transcritical bifurcation is the most fundamental switch in epidemiology. Imagine the DFE as a stable main road. Provided $\mathscr{R}_0 < 1$, all small outbreaks will naturally return to this main path and disappear. Exactly at the point $\mathscr{R}_0 = 1$, a bifurcation appears: the main road DFE becomes unstable, and a new road—i.e., the endemic condition—emerges and becomes stable. The epidemic will now follow this new path. To mathematically prove the existence of this intersection, we need to analyze the stability of the DFE point. The Jacobian matrix of System (1) evaluated at Ω_0 is expressed as follows.

$$\mathbf{J}(\Omega_0) = \begin{bmatrix} -k_1+1 & 0 & 0 & \frac{k_2\mu(-k_3k_4+\tau_1\tau_2)\mathscr{R}_0}{(\tau_1 q+k_4)((p\varphi_1+k_2)\mu+\varphi_1\varphi_2 r)} & \frac{k_2\mu(-k_3k_4+\tau_1\tau_2)\mathscr{R}_0 q}{(\tau_1 q+k_4)((p\varphi_1+k_2)\mu+\varphi_1\varphi_2 r)} & \rho \\ \varphi_1 & -k_2+1 & 0 & \frac{\varphi_1\mu(-k_3k_4+\tau_1\tau_2)\mathscr{R}_0 p}{(\tau_1 q+k_4)((\mu p+r\varphi_2)\varphi_1+\mu k_2)} & \frac{\varphi_1\mu(-k_3k_4+\tau_1\tau_2)\mathscr{R}_0 qp}{(\tau_1 q+k_4)((\mu p+r\varphi_2)\varphi_1+\mu k_2)} & 0 \\ 0 & \varphi_2 & -\mu+1 & \frac{\varphi_1\varphi_2(-k_3k_4+\tau_1\tau_2)\mathscr{R}_0 r}{(\tau_1 q+k_4)((\mu p+r\varphi_2)\varphi_1+\mu k_2)} & \frac{\varphi_1\varphi_2(-k_3k_4+\tau_1\tau_2)\mathscr{R}_0 qr}{(\tau_1 q+k_4)((\mu p+r\varphi_2)\varphi_1+\mu k_2)} & 0 \\ 0 & 0 & 0 & \frac{(-k_3q-\mathscr{R}_0\tau_2+q)\tau_1+k_4(1+(\mathscr{R}_0-1)k_3)}{\tau_1 q+k_4} & \frac{(-\tau_2(\mathscr{R}_0-1)\tau_1+k_3k_4\mathscr{R}_0)q+k_4\tau_2}{\tau_1 q+k_4} & 0 \\ 0 & 0 & 0 & \tau_1 & -k_4+1 & 0 \\ 0 & 0 & 0 & \gamma_n+\gamma_m & \gamma_n & 1-\rho-\mu \end{bmatrix}.$$

In addition, the eigenvalues of $\mathbf{J}(\Omega_0)$ are given as

$$\beta_1 = -\mu+1, \qquad \beta_3 = \frac{l_1+\sqrt{l_2}}{2(q\tau_1+k_4)}, \quad \beta_5 = -k_2+1,$$

$$\beta_2 = 1-\rho-\mu, \quad \beta_4 = \frac{l_1-\sqrt{l_2}}{2(q\tau_1+k_4)}, \quad \beta_6 = -k_1+1,$$

where $l_1 = (-k_3q-k_4q-\mathscr{R}_0\tau_2+2q)\tau_1-k_4^2+(2+(\mathscr{R}_0-1)k_3)k_4$ and $l_2 = (k_3k_4-\tau_1\tau_2)^2\mathscr{R}_0^2+4(\tau_1 q+k_4)(k_3k_4-\tau_1\tau_2)(\tau_1 q-\frac{k_3}{2}+\frac{k_4}{2})\mathscr{R}_0+(\tau_1 q+k_4)^2(4\tau_1\tau_2+(k_3-k_4)^2)$. In this case, setting $\mathscr{R}_0 = 1$ makes $\beta_3 = \frac{l_1+\sqrt{l_2}}{2(q\tau_1+k_4)} = 1$, which confirms the transcritical bifurcation [29].

Proposition 3 System (1) undergoes a transcritical bifurcation at $\mathscr{R}_0 = 1$.

3.2.3 *Dual threshold bifurcation: manifestations*

Combining the analyses of the saddle-node and transcritical bifurcations, the system exhibits dynamics that are far more complex than simple forward or backward bifurcations. We refer to this as the dual threshold bifurcation because it reveals critical transitions governed by two distinct thresholds or gates, each of which leads to drastically different epidemic outcomes. Dual threshold bifurcation becomes a critical point where the system can either jump to a severe

epidemic state or remain under control, depending on two different thresholds. This bifurcation manifests in two distinct types, each of which profoundly impact pandemic control.

3.2.3.1 *Dual threshold bifurcation type I*

This type of bifurcation arises from the interplay of the transcritical bifurcation at $\mathscr{R}_0 = 1$ with specific saddle-node conditions that allow for multiple EEs even when $\mathscr{R}_0 < 1$. From Corollary 1 and Propositions 1, 2, and 3, the system displays a backward bifurcation when $C > 0$ and $B < 0$, and a forward bifurcation when $C < 0$ and $B < 0$. These standard bifurcations are formally described as follows.

Corollary 2 System (1) undergoes a backward bifurcation at $\mathscr{R}_0 = 1$ if $C > 0$ and $B < 0$, and undergoes a forward bifurcation if $C < 0$ and $B < 0$.

Coefficients B and C are not abstract numbers; they are complex combinations of various model parameters (e.g., vaccination rate, quarantine effectiveness, and recovery rate). The sign of these coefficients effectively determines the shape of the epidemic curve around the critical point $\mathscr{R}_0 = 1$. For example, the condition $C > 0$ often indicates the presence of mechanisms (such as reinfection o waning immunity) that support disease persistence even at low transmission levels, potentially leading to dangerous backward bifurcations.

These basic behaviors are illustrated in Figure 1a and 1b, showing that a forward bifurcation indicates controllable disease spread, and a backward bifurcation indicates more complex, difficult-to-control dynamics where the force of infection α can jump significantly. A more complex scenario, referred to as the dual threshold bifurcation type I, arises when $B > 0$, $C < 0$, and $B^2 + 3AC > 0$. Under these conditions, Proposition 1 indicates the potential for three EE points, leading to two saddle-node bifurcations.

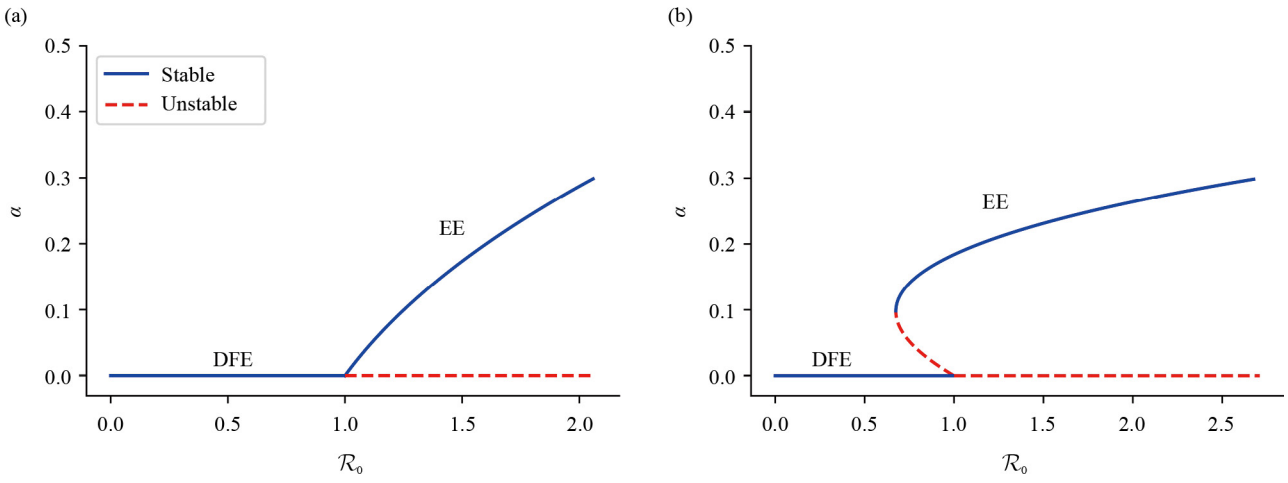

Figure 1. (a) Forward bifurcation, (b) Backward bifurcation

Corollary 3 System (1) undergoes a Dual Threshold Bifurcation (Forward-Backward bifurcation type I) at $\mathscr{R}_0 = 1$ if $B > 0$, $C < 0$, and $B^2 + 3AC > 0$.

As shown in Figure 2, the dual threshold bifurcation type I is more perilous than a standard backward bifurcation. Here, the disease spread initially increases slowly as $\mathscr{R}_0$ approaches and exceeds 1; However, the force of infection α escalates drastically once $\mathscr{R}_0$ exceeds $h\left(\frac{-B+\sqrt{B^2-3AC}}{3A}\right)$. This sudden, large surge implies that the system can unexpectedly jump into a high-transmission state, even when $\mathscr{R}_0$ is seemingly under control. Thus, control efforts must be extremely aggressive, continuously suppressing $\mathscr{R}_0$ below $h\left(\frac{-B-\sqrt{B^2-3AC}}{3A}\right)$, to prevent this faster and more significant increase in the transmission rate.

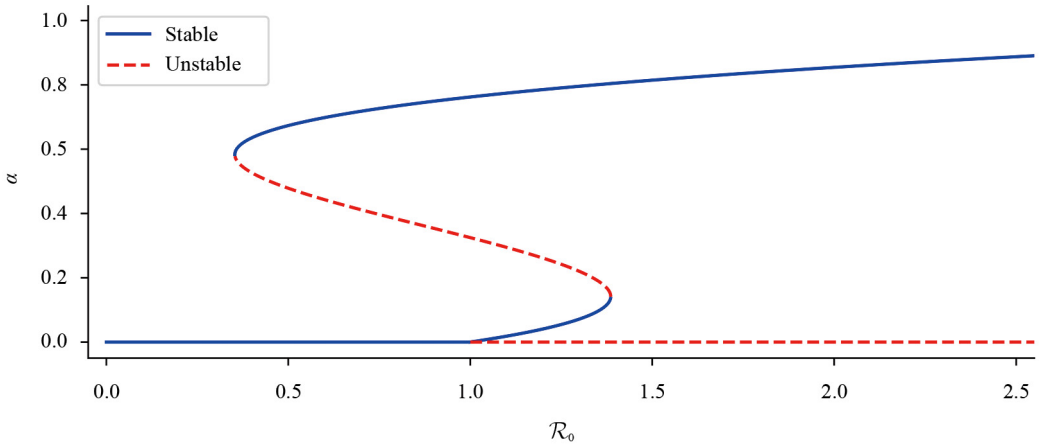

Figure 2. Dual threshold bifurcation type I

3.2.3.2 *Dual threshold bifurcation type II*

This type of bifurcation specifically addresses the system's behavior when the number of infected individuals I_t exceeds the medical resource threshold I_b. For this analysis, we transition the bifurcation diagram to illustrate the infection rate λ versus the number of infected individuals I to better depict the shifts in the system's conditions from $I_t \leq I_b$ to $I_t > I_b$.

We also explore the EE Ω_2, derived from the quartic Equation (5) (which is applicable when $I_t > I_b$), for potential bifurcations. Similar to Proposition 2, the saddle-node bifurcations occur at the extremum points of this equation. The first derivative of Equation (5), i.e., $h_1'(I_2) = 4A_1I_2^3 + 3B_1I_2^2 + 2C_1I_2 + E_1$, reveals these extrema. The general solutions for $h_1'(I_2) = 0$ are given as follows [32]:

$$I_{2_1} = y_1 - \frac{b}{3}, \qquad I_{2_2} = y_2 - \frac{b}{3}, \qquad I_{2_3} = y_3 - \frac{b}{3}, \tag{6}$$

where

$$y_1 = L_1 + L_2, \quad y_2 = \omega L_1 + \omega^2 L_2, \quad y_3 = \omega^2 L_1 + \omega L_2,$$

with

$$L_1 = \sqrt[3]{-\frac{n}{2} + \sqrt{N}}, \qquad L_2 = \sqrt[3]{-\frac{n}{2} - \sqrt{N}},$$

$$\omega = -\frac{1}{2} + \frac{1}{2}\sqrt{3}i, \qquad \omega^2 = -\frac{1}{2} - \frac{1}{2}\sqrt{3}i,$$

$$N = \left(\frac{m}{3}\right)^3 + \left(\frac{n}{2}\right)^2,$$

$$m = c - \frac{bc}{3}, \quad n = e - \frac{bc}{3} + \frac{2b^3}{27}.$$

and the coefficients of $h_1'(I_2)$ are $h_1'(I_2) = I_2^3 + bI_2^2 + cI_2 + e$ with $b = \frac{3B_1}{4A_1}$, $c = \frac{C_1}{2A_1}$, and $e = \frac{E_1}{4A_1}$.

Unlike Equation (3), the parameter λ in Equation (5) influences up to four coefficients, thereby causing the extremum points to shift dynamically. Note that an additional condition is required for a saddle-node bifurcation to occur, i.e., the selected extremum point (I_e) must also be a root of Equation (5), meaning $h_1(I_e) = 0$. We select the largest real solution of $h_1'(I_2)$, i.e., I_{2_1}, as the candidate for the saddle-node point, which yields the following proposition.

Proposition 4 Equation (5) undergoes a saddle-node bifurcation at $I_2 = y_1 - \frac{b}{3}$ if $h_1\left(y_1 - \frac{b}{3}\right) = 0$.

This condition defines the dual threshold bifurcation type II, which occurs when this saddle-node bifurcation point is located above the medical resource threshold I_b.

Corollary 4 System (1) undergoes a dual threshold bifurcation (forward-backward bifurcation type II) when $h_1\left(y_1 - \frac{b}{3}\right) = 0$ and $y_1 - \frac{b}{3} > I_b$.

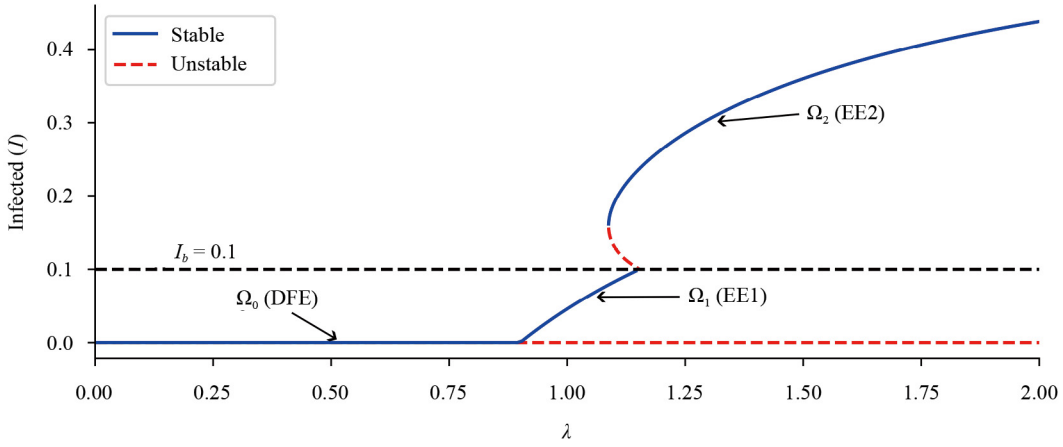

Figure 3. Dual threshold bifurcation type II

As shown in Figure 3, the dual threshold bifurcation type II demonstrates how exceeding the medical resource threshold I_b drastically alters the dynamics of the epidemic. Here, when the infected population I exceeds I_b, the system experiences a sudden, sharp increase in the infection rate λ. This surge reflects the real-world consequence of overwhelmed healthcare systems, i.e., once capacity is exceeded, the transmission of the disease accelerates, potentially becoming uncontrollable. Thus, understanding this medical resource threshold is crucial in terms of preventing exponential disease spread. The aforementioned mathematical analysis reveals the existence of complex critical points (bifurcations) in our model. Although not merely out of mathematical curiosity, these points have profound real-world implications for designing pandemic policies. In the next section, we translate these dynamic findings into concrete lessons for policymaking.

3.3 *Policy implications and pandemic ironies*

The results of the bifurcation analysis (Section 3.2) highlight the intricate nature of pandemic dynamics, revealing that even slight shifts in parameters can drastically alter the spread of the disease due to the dual threshold bifurcation (types I and II). In the following, we examine the significant policy implications of this phenomenon, focusing on two key aspects, i.e., the critical importance of swift and decisive initial policies and the necessary adaptation of intervention

strategies once a region enters an endemic state. The discussion also considers the inherent ironies within these dynamics, which frequently defy conventional comprehension and complicate disease control efforts.

3.3.1 *Dual threshold bifurcation type I: irony of "Life's Gamble" in the early phase*

In the early phase of a pandemic, the model shows that the dual threshold bifurcation type I dynamics are crucial before the infected cases I_t exceed the medical capacity I_b. This represents the initial spread where the type I bifurcation diagram reveals a single relevant EE when $I_t \leq I_b$, which indicates that the healthcare system is not yet critically overwhelmed. A key feature of the type I bifurcation is the presence of two critical thresholds, i.e., $\mathscr{R}_0^{\text{left}}$ and $\mathscr{R}_0^{\text{right}}$, which define the hysteresis zone. This hysteresis zone means that the path to suppress the outbreak differs from the path when the outbreak emerges. For example, to exit a high endemic state, we might need policies that are considerably stricter (suppressing $\mathscr{R}_0$ to 0.7) than the threshold when the outbreak first emerged ($\mathscr{R}_0 = 1$). In this zone, the system's behavior depends on both the current parameters and its history.

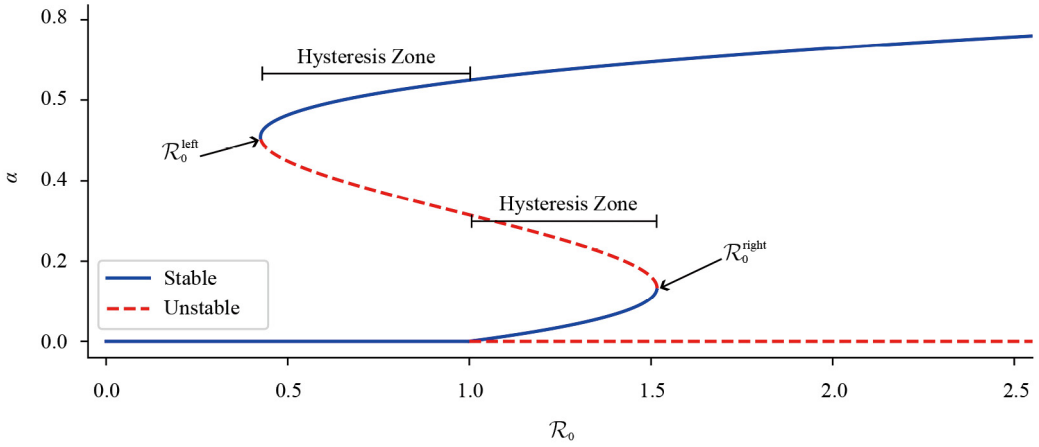

Figure 4. Hysteresis zone in dual threshold bifurcation type I

Within the hysteresis zone, multiple stable equilibrium points coexist, i.e., a stable DFE, a stable EE, and an unstable EE (from $\mathscr{R}_0^{\text{left}}$ to $\mathscr{R}_0 = 1$). From $\mathscr{R}_0 = 1$ to $\mathscr{R}_0^{\text{right}}$, two stable EEs (low and high) and an unstable EE can appear (Figure 4), and this coexistence makes the system highly unpredictable. Depending on the initial conditions or random fluctuations, the system can stabilize at either the ideal DFE or a persistent EE, thereby leading to the endemic trap, which is a sustained endemic condition despite a mathematical path to disease freedom, causing significant uncertainty. Systems that fall into an endemic trap will experience a situation where the outbreak is difficult to eliminate and persists in the population (becoming endemic), even when $\mathscr{R}_0$ is already below 1.

Thus, bold and swift health policies are critically essential during the early phase of a pandemic. The hysteresis zone is a costly real-world scenario, and early COVID-19 policy debates in Indonesia highlight this dilemma. Failing to act quickly pushes the system into this unpredictable zone, drastically increasing social and economic costs, including prolonged online activities, strain on tourism and small and medium enterprises, and psychological burdens.

Thus, prompt and bold government interventions are required to escape the endemic trap. Hesitation can push the system to pass the right-side threshold, thereby causing extreme case surges and overwhelming medical resources beyond I_b. Conversely, aggressive interventions, e.g., strict lockdowns, mass quarantines, extensive contact tracing/isolation, and early widespread vaccination, seek to suppress the spread of the disease, decisively pushing the system toward a stable DFE. This is the irony of "Life's Gamble". This is defined as a zone of uncertainty where the success of an intervention is at stake: the system can be stable under good (disease-free) or bad (endemic) conditions, although the parameters are

the same. In the early phase of a pandemic, authorities face high-stakes decisions that will determine the epidemic's fate: elimination or an uncontrolled pandemic.

In real-world scenarios, becoming trapped in an endemic state or hysteresis zone is evident from recurring drastic case surges (waves), the emergence of transmissible new variants, repeatedly overwhelmed healthcare systems, and fundamental, long-term shifts to online public activities. These are concrete manifestations of the significant social and economic costs, and the reality of the endemic trap highlights the rigid need to escape the hysteresis zone, reinforcing why aggressive interventionist health policies must be adopted quickly and boldly in the early phase of a pandamic. For example, this can be seen in the UK and Sweden, where the initial hesitation in responding to the pandemic had severe consequences. In England, the delay in implementing the first lockdown caused the initial wave of COVID-19 to surge uncontrollably, overwhelming hospitals and leading to thousands of preventable deaths [33]. Sweden, which chose not to implement a strict lockdown and relied solely on voluntary recommendations, experienced a markedly higher per capita death rate than its Nordic neighbors, particularly in severely affected nursing homes [34]. These two cases demonstrate that delays and hesitation in the early stages of the pandemic can trap countries in a cycle of recurring waves of infection, highlighting the importance of swift and decisive intervention before the situation spirals out of control.

In real-world scenarios, becoming trapped in an endemic state or hysteresis zone is evident from recurring drastic case surges (waves), the emergence of transmissible new variants, repeatedly overwhelmed healthcare systems, and fundamental, long-term shifts to online public activities. These are concrete manifestations of the significant social and economic costs, and the reality of the endemic trap highlights the rigid need to escape the hysteresis zone, reinforcing why aggressive interventionist health policies must be adopted quickly and boldly in the early phase of a pandemic. If conditions are allowed to descend into the endemic trap, they will inevitably produce two costly consequences, namely the substantial price of falling into the trap and the equally substantial cost of remaining within it.

The first consequence is the cost of delayed action, clearly illustrated by the experiences of the UK and Sweden. The initial hesitation in their pandemic responses resulted in severe consequences. In England, the delay in implementing the first lockdown caused the initial wave of COVID-19 to surge uncontrollably, overwhelming hospitals and leading to thousands of preventable deaths [33]. Sweden, which chose not to implement a strict lockdown and relied solely on voluntary recommendations, experienced a markedly higher per capita death rate than its Nordic neighbors, particularly in severely affected nursing homes [34]. Both cases demonstrate that delays in the early stages of a pandemic impose significant social and economic costs, ultimately locking countries into endemic conditions. A rapid shift from a DFE to a higher EE leads to a surge in cases, straining health systems and increasing elimination costs. Such a rapid shift from a DFE to a higher EE, which triggers case surges and strains health systems, marks the onset of a self-perpetuating cycle of recurrent infection waves.

Another consequence is the "cost of remaining" in the endemic trap, which clearly happens in many high-income countries that have adopted a "living with the virus" strategy. These countries are locked at a persistent EE. The trap lies in institutionalized, recurring expenditures—multibillion-dollar booster campaigns, subsidized testing programs, and sustained productivity losses—despite an $\mathscr{R}_0$ that is technically under control. This costly stability illustrates the endemic trap: a system fixed at EE where social and economic burdens persist, underscoring the urgent need to push $\mathscr{R}_0$ beyond the threshold $\mathscr{R}_0^{\text{left}}$.

3.3.2 *Dual threshold bifurcation type II: irony of "choosing between low and high endemic epidemic"*

Shifting from early pandemic dynamics (type I), the dual threshold bifurcation type II becomes relevant when the infected cases I_t exceed the medical capacity I_b, indicating a strained or overwhelmed healthcare system. This analysis utilizes the infection rate λ as a control parameter to reflect the changes in the disease transmission.

The type II bifurcation diagram shows an evolving progression. Initially, only the DFE is stable (e.g., from $\lambda = 0$ to $\lambda = 1.156$). As λ increases from 1.156 to λ_{right}, the first EE (EE1) emerges and stabilizes, signaling persistent disease. Crucially, beyond λ_{right}, a backward bifurcation-like transition leads to the emergence of a second EE (EE2). Here, a new hysteresis zone is formed between λ_{left} (between 1.156 and λ_{right}) and λ_{right} (Figure 5).

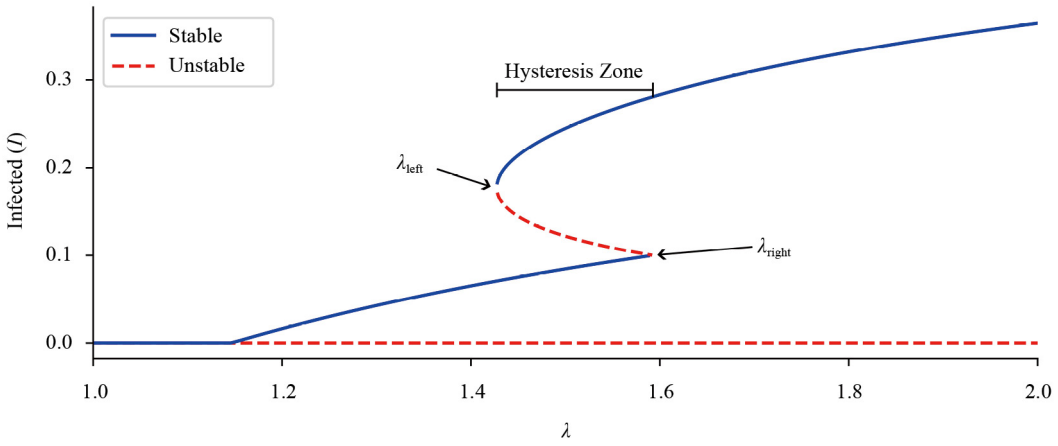

Figure 5. Hysteresis zone in dual threshold bifurcation type II

Within this type II hysteresis zone, the system exhibits complex bistability with a stable EE1, a stable EE2 (i.e., higher infection), and an unstable EE2. Significantly, the boundary that determines whether the system gravitates toward EE1 (low endemic) or EE2 (high endemic) is the medical capacity threshold I_b rather than the unstable EE. If I_t is below I_b, the system trends toward EE1; however, if I_t exceeds I_b, even if mathematically below the unstable EE, the system will still be attracted to the high EE2, thereby making epidemic prediction very difficult unless I_t is pushed below I_b. Beyond λ_{right}, only the EE2 remains stable, indicating a high level of infection that is difficult to control.

Type II interpretation is highly relevant to prolonged pandemics. Unlike type I, which focuses on the early risks of an endemic trap when capacity is not exceeded, type II describes a deeper crisis where healthcare systems are overwhelmed or collapsing. Indonesia's multiple COVID-19 waves, particularly the mid-2021 surge of the Delta variant, with full hospitals and strained resources, exemplify the system being in the type II hysteresis zone, having exceeded I_b.

In this severe zone, aggressive intervention is mandatory. However, the choice remains between two endemic conditions, i.e., stabilizing at a low level (EE1) or a high level (EE2) that overwhelms the system. Thus, authorities face a new phenomenon: the "Irony of Choosing between a Low and High Endemic Epidemic".

Successfully pushing the system left past λ_{left} through aggressive measures (e.g., emergency lockdowns, rapid vaccination efforts, drastic increases in hospital capacity, and strict mobility curbs) allows the system to exit the hysteresis zone. However, unlike type I, which offers a stable DFE, type II success only returns the system to a stable EE1, which implies that while extreme surges are averted and control is regained at a lower level, the disease persists, and achieving a DFE becomes a much longer, harder battle—a stark reminder that delayed responses can eliminate the short-term disease-free option.

Nonetheless, this nonideal choice is superior to the worst-case scenario. If interventions fail or are insufficient, the system will be pushed past λ_{right}, stabilizing only at EE2, representing a very high, uncontrolled, and resource-overwhelming epidemic. Thus, at this stage, policy shifts from disease prevention to choosing between two endemic scenarios, i.e., accepting a low-level, draining pandemic or succumbing to a high-level, paralyzing one. Here, intervention is about maximal mitigation to guide the system toward the least detrimental outcome and prevent total collapse rather than disease elimination.

3.3.3 *Two interconnected ironies: the evolving challenge of pandemics*

The two ironies from dual threshold bifurcation types I and II represent the sequential, time-linked phases of pandemic challenges. Type I's "Life's Gamble" irony occurs in the early phase, where the number of infected cases is less than the medical capacity I_b. Here, authorities face a critical choice, i.e., act swiftly and boldly for a DFE or risk an unpredictable hysteresis zone where the epidemic can surge, even with $\mathscr{R}_0 < 1$.

Indonesia's early 2020 COVID-19 experiences illustrate this situation. Government hesitancy regarding large-scale social restrictions and other responses demonstrated that hesitation or insufficient early action frequently proved fatal. When the initial responses were not sufficiently aggressive to suppress transmission drastically, the system gradually or suddenly surpassed the type I hysteresis thresholds, thereby leading to a prolonged endemic trap.

If early aggressive actions are delayed or these efforts fail, the pandemic system will likely transition to type II conditions, where the infected cases I_t exceed the medical capacity I_b. At this point, the epidemic dynamics worsen and options diminish. Here, the path to a stable DFE, present in type I, vanishes, and the irony shifts from "Life's Gamble" to the "Irony of Choosing between a Low and High Endemic Epidemic". Under these conditions, rather than elimination, the clear priority is managing the severity of the endemic state, where even aggressive interventions only lead to a lower EE, not DFE.

Indonesia's mid-2021 second wave, dominated by the Delta variant and caused healthcare collapse, tragically exemplifies this type II transition. Even with persistently high numbers of cases, the focus shifted from eliminating the virus to suppressing cases to prevent overwhelming the healthcare system.

Thus, the temporal link between these bifurcations highlights a stark lesson: speed and decisiveness in defining and implementing early pandemic policies are crucial. In this phase, failure means not only a lost opportunity but also pushes society into a more difficult, costly scenario with limited options, where the fight evolves from total elimination to maximum damage mitigation.

3.4 *Adapting intervention strategies in an endemic trap: risks and the irony of consequences*

When early pandemic policies fail, and the system is entangled in the endemic trap, signaling the missed opportunity for a DFE, the nature of the challenge shifts dramatically. Here, the focus is on adapting strategies to achieve a more controlled state (rather than total elimination), acknowledging the significant risks of failure. The following discussions and simulations assume a dual threshold bifurcation type II scenario, representing an advanced pandemic phase where the medical capacity is already exceeded or severely threatened. This sets the stage for understanding the complex journey within these dynamics.

3.4.1 *Parameterization for numerical simulations*

The numerical simulations presented in this section serve as an illustrative proof-of-concept for the analytical findings of the bifurcation analysis. The primary goal is not to provide quantitative predictions for a specific epidemic but rather to demonstrate the existence and explore the qualitative behavior of the complex dynamics, such as the endemic traps and hysteresis zones, that our model can exhibit.

Table 2. Baseline parameter values used for numerical simulations

Parameter	Value	Source/Rationale
Parameters varied in analysis:		
λ	1.47	Calibrated to place the system within the desired hysteresis zone, enabling the simulation of scenarios like the rebound trap.
Parameters based on previous work and literature:		
p	0.590071	Derived from vaccine efficacy calculations [15].
r	0.180143	Derived from vaccine efficacy calculations [15].
q	0.05	Derived from quarantine efficacy calculations [15].
d	0.02	Derived from vaccine mortality reduction calculations [15].
ρ	0.0065	Based on studies of waning immunity [35].

Table 2. (cont.)

Parameter	Value	Source/Rationale
Parameters selected to demonstrate key dynamics:		
φ_1	0.2	Numerically selected as part of the baseline parameter set that produces
φ_2	0.1	the rich bifurcation structures analyzed in this paper.
τ_1	0.15	These values were identified through systematic simulation to find a
τ_2	0.05	region in the parameter space where the pandemic ironies
γ_n	0.0015	are clearly observable.
γ_m	0.5	
ζ	0.001	
μ	0.3	
I_b	0.1	Set to a critical threshold (10% of total population) that clearly separates the low and high endemic states for the type II bifurcation.

The parameter values used in the following simulations (Table 2) are selected hypothetically but are within biologically plausible ranges. These values were determined through extensive preliminary simulations to find a parameter set that clearly exhibits the specific bifurcation structures and pandemic ironies that are the central focus of this study.

3.4.2 *Trapped in a high endemic state: an unavoidable dilemma*

We distinguish two endemic conditions: (i) high endemic state, where the number of infections is stable at a high level and exceeds medical capacity ($I > I_b$), and (ii) low endemic state, where the disease persists but at a stable and controlled level below medical capacity ($I < I_b$). This scenario describes a pandemic system trapped in a stable high endemic state within the hysteresis zone ($\lambda_{\text{left}} < \lambda < \lambda_{\text{right}}$), as shown in Figure 6. This is a critical and unsustainable situation involving consistently high positive cases, severely overwhelmed healthcare systems (full hospitals, scarce beds, and exhausted staff), and widespread societal suffering, including surging mortality, economic strain from restrictions, and deteriorating public mental health.

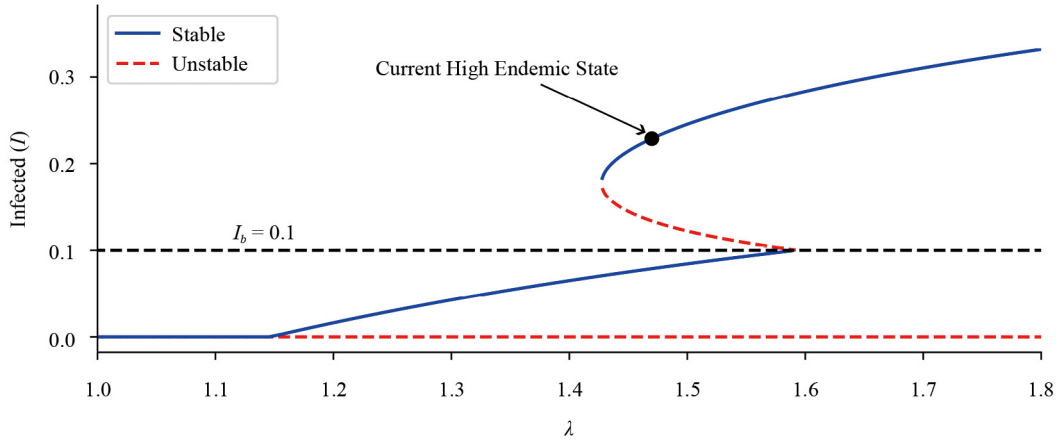

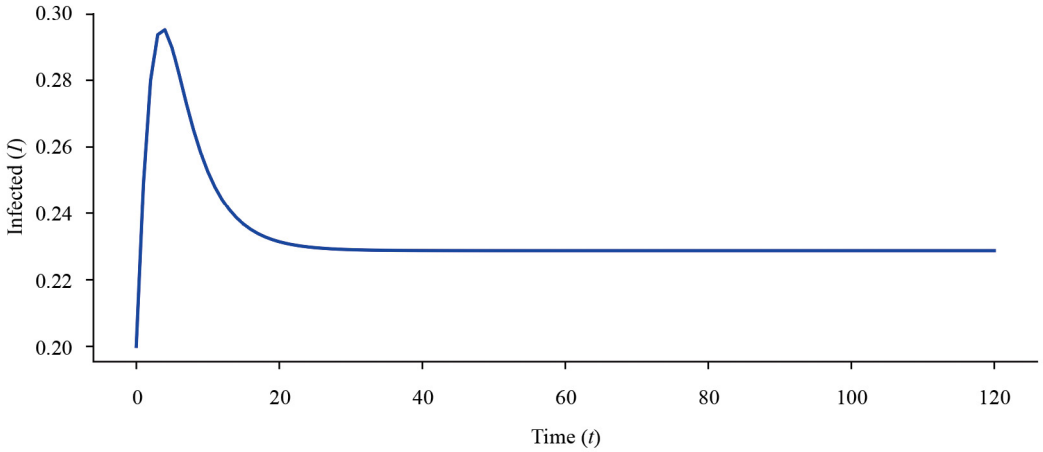

Figure 6. High endemic state

Crucially, in the dual threshold bifurcation type II, being trapped in a high endemic state within the hysteresis zone indicates that the infected cases I_t have surpassed the medical capacity threshold I_b; thus, I_b functions as a real boundary that dictates the system's attraction. Simulations confirm that in this high endemic state, the system stabilizes at a high EE without natural remission and is effectively "comfortable" at a high spread level. However, the devastating long-term impacts require urgent intervention. Here, the immediate goal is to suppress the number of cases to bring I_t below I_b, thereby enabling a shift toward a more manageable low endemic state, which is an absolute prerequisite for any further efforts to control the pandemic.

3.4.3 *Pushing toward a low endemic state: the rebound trap and cost of failure*

To combat a stable high endemic state, governments must significantly reduce infection levels (I_t). The implementation of self-quarantine rules is an initial measure that can directly suppress I_t, and greater compliance further diminishes the system's contribution to I_t. This aligns with System (1), which indicates that a lower q reduces transitions into compartment I. If this measure proves insufficient, governments must adopt comprehensive interventions. These may include emergency regional quarantines, aggressive contact tracing, mass testing, rapid vaccination, and strict enforcement of health protocols. The ultimate goal is to reduce I_t below the medical capacity threshold (I_b), enabling a sustainable transition to a manageable low endemic state.

A rebound trap is defined as a phenomenon where interventions that appear to successfully suppress the number of cases fail to reach a critical threshold, causing the system to automatically return (rebound) to a high endemic state once the intervention is relaxed. To validate this, numerical simulations were performed, where the initial system values were varied to answer policymakers' "what if" questions regarding the effectiveness of different interventions. Note that these simulations assumed that the other parameters, e.g., λ, remained, modeling interventions that reduce the case numbers without permanently altering the viral transmission.

Starting from a stable high endemic state, a simulated 5% daily case reduction for seven days (lockdown), representing aggressive intervention, was applied. The results demonstrated that an 8% or less daily reduction was insufficient because the system rebounded to the high endemic state, as shown in Figure 7. These findings demonstrate that half-hearted efforts, even if they temporarily reduce I_t, fail if they do not consistently push I_t below I_b. In the type II hysteresis zone, I_b acts as an "invisible wall", ensuring the dominant pull toward the high endemic state if I_t remains above I_b.

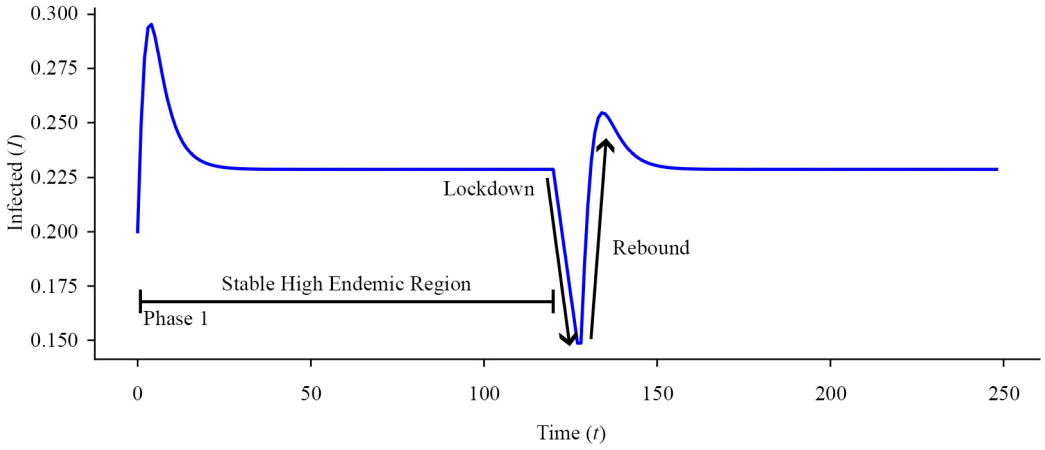

Figure 7. Rebound trap: pulled back to high endemicity

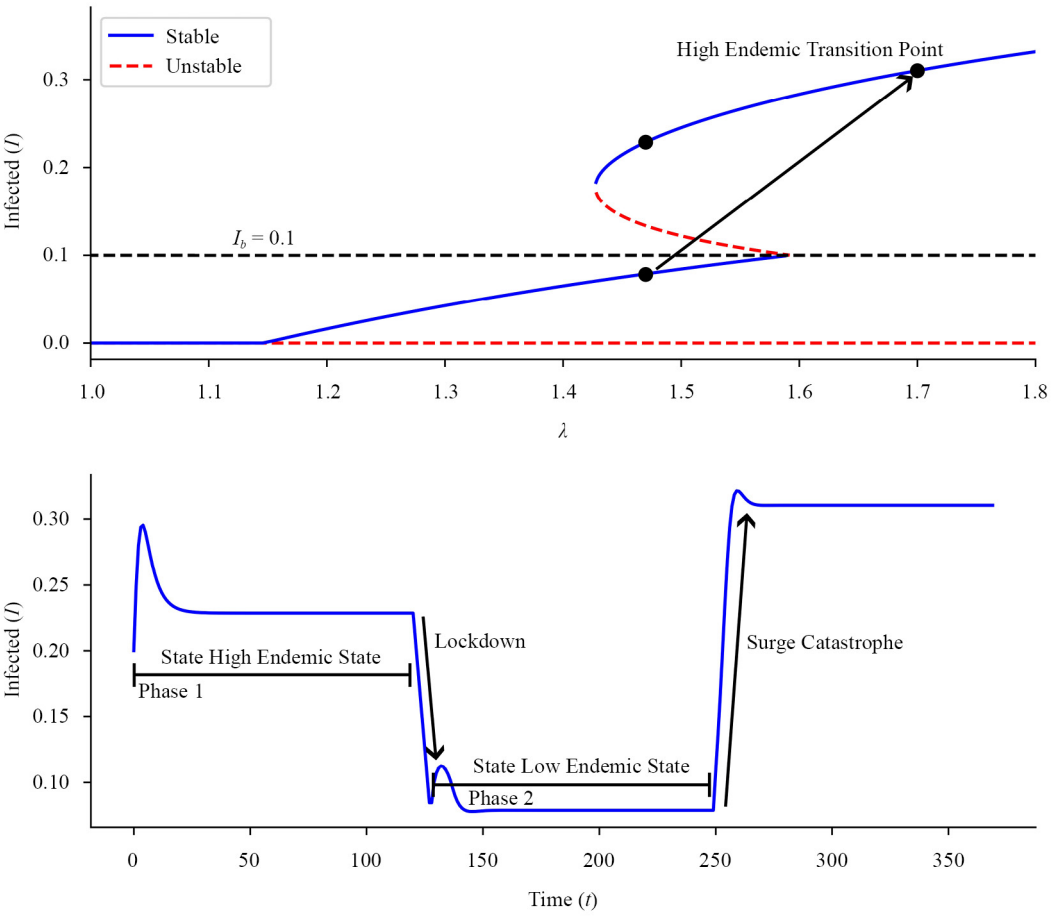

Figure 8. Successful aggressive intervention: suppressing high endemicity to a stable low endemic state

We found that only a simulated 9% daily case reduction over seven consecutive days moved the system to a stable low endemic state (Figure 8), which implies that aggressive interventions in a high endemic state must achieve a daily case reduction of at least 9% (based on the simulation parameters) to improve the situation.

Indonesia's COVID-19 pandemic involved multiple waves (Figure 9) that exhibited this rebound phenomenon when restrictions were eased or compliance dropped before I_b was truly controlled. A similar phenomenon was observed in European countries during the summer of 2020, when France, Germany, Belgium, and the Czech Republic eased restrictions after the first wave, which then triggered a considerably more severe second wave in the autumn [36]. In the United States, public euphoria emerged after the initial vaccine rollout in early 2021, leading to the lifting of mask mandates and the easing of health protocols, only to be followed by a large surge in cases due to the Delta variant [37]. The immense sacrifices, i.e., economic downturns, lost livelihoods, psychological burdens, and exhausted healthcare workers, became futile with each rebound. This "second trap" depletes limited resources and erodes public trust in government policies. Successfully pushing cases below I_b is not the end goal, but a vital prerequisite to advance to the next phase of pandemic control.

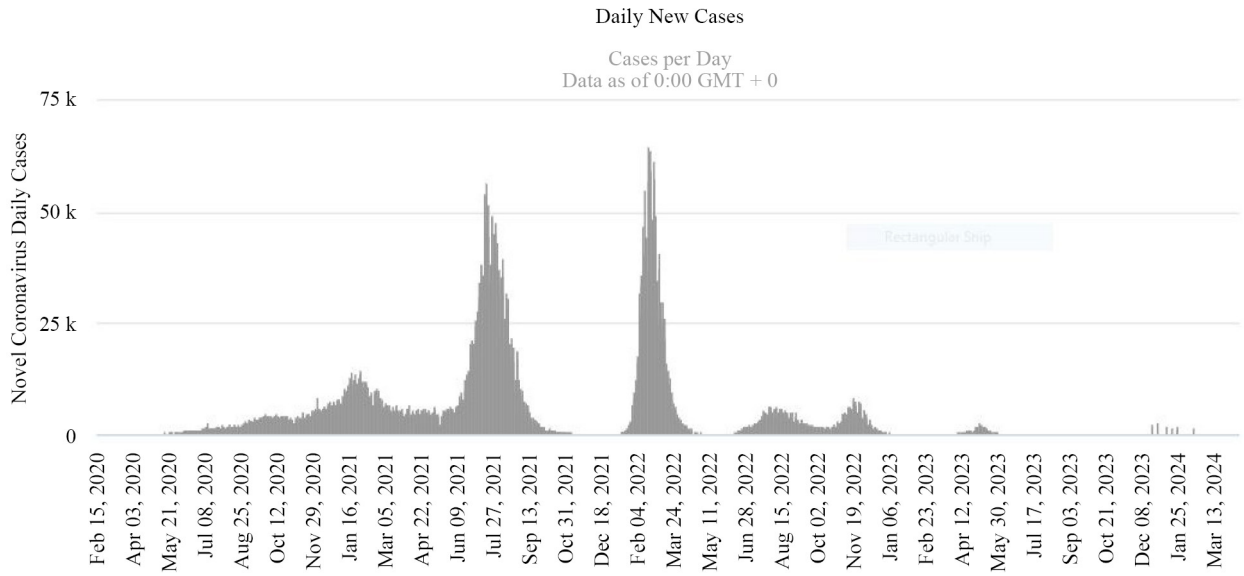

Figure 9. Daily COVID-19 cases in Indonesia [38]

3.4.4 *Suppressing to low endemic state: false comfort zone*

After exhausting efforts and encountering potential setbacks, authorities may suppress infected cases I_t below the medical capacity threshold I_b, thereby achieving a stable low endemic state. This partial success brings relief in the form of drastically fewer cases, reduced strain on the healthcare system, and a return to perceived normalcy as restrictions ease; however, this also creates an illusion of full control. This condition is defined as a false comfort zone, which is a stable but vulnerable low endemic state. Although the number of cases appears controlled, the system remains in a hysteresis zone, meaning that even a small disruption can rapidly trigger a return of the epidemic to high-endemic levels.

Our model reveals a new irony, i.e., "false comfort". While preferable to a high endemic state, if the virus transmission parameter λ remains within the hysteresis zone ($\lambda_{\text{left}} < \lambda < \lambda_{\text{right}}$), this low endemic condition represents a false comfort zone, in which the system remains highly vulnerable. The results of numerical simulations highlight this vulnerability. Here, after reaching a low endemic state, a minor disturbance (e.g., a 6% daily increase in I_t for only three days) is sufficient to push I_t slightly above I_b, dramatically pulling the system back into a stable high endemic state, as shown in Figure 10.

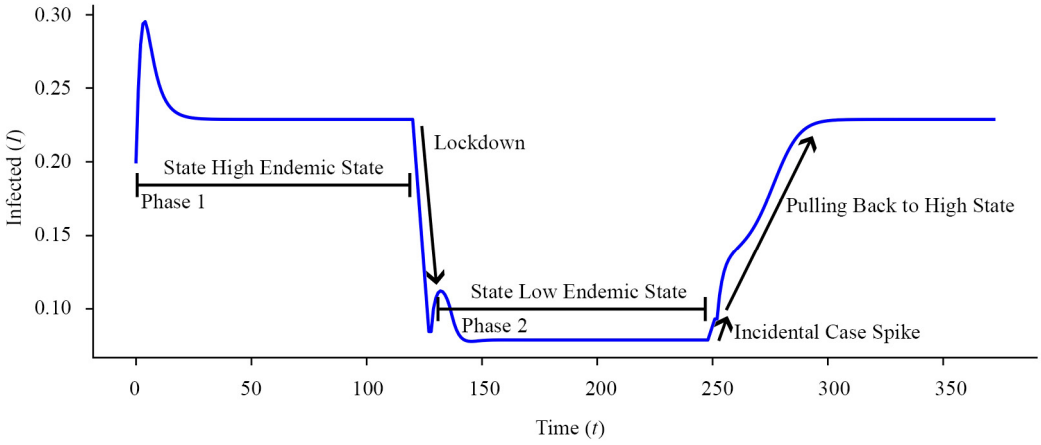

Figure 10. Incidental spike triggers return to high endemicity

The aforementioned phenomenon was reflected in India's real-world experience in early 2021. After the first wave of COVID-19 subsided, the number of daily cases in several parts of India plummeted, creating a widespread perception that the pandemic was nearly over. Social and economic activities reopened, health protocols were relaxed, and public vigilance decreased [39]. However, this situation proved fragile when the highly contagious Delta variant began to spread, triggering a devastating second wave. Hospitals were overwhelmed, oxygen supplies dwindled, and death rates soared drastically, even leading to many patients dying due to a lack of care. This event demonstrates that even after reaching a low endemic state, a marginal complacency can lead to a major disaster.

Note that this stark disparity is critical, i.e., achieving a low endemic state requires aggressive, sustained effort (e.g., seven consecutive days of a 9% daily case reduction); however, even a minimal lapse (three days of a 6% increase) can reverse all progress made. This demonstrates the fragility of the low endemic condition, where immense social and economic investments can be undone rapidly. This irony of false comfort is a crucial lesson. In other words, even when case numbers appear low, constant vigilance and swift action are paramount because complacency can nullify all sacrifices.

3.4.5 *Threat of sudden attack: explosive waves and hope for consistency*

Even in a seemingly stable low endemic state, a constant threat persists from shifts in the transmission parameter λ. Such shifts can be triggered by various factors, e.g., the emergence of more transmissible variants (e.g., the Omicron vs. Delta variants), premature policy easing due to complacency or public euphoria, or a drastic decline in adherence to health protocols once a false sense of security is established.

Vaccination programs play a critical role in sustaining a low EE by strengthening system resilience against sudden shifts in λ. While vaccination does not directly reduce the transmission parameter in System (1), maintaining widespread and recurrent immunization can mitigate the risk of explosive rebounds by buffering the population against severe outcomes. In this sense, vaccination acts as a stabilizing mechanism: although its immediate effect on λ may be indirect, the cumulative impact of sustained large-scale immunization inevitably contributes to lowering infection dynamics and reducing the likelihood of catastrophic surges.

The consequences of such behaviors are dramatic and represent a worst-case scenario. For example, if λ suddenly exceeds λ_{right} (the point at which the low endemic stable equilibrium vanishes from the hysteresis zone), the system will rapidly surge back to a high endemic state. Simulation results demonstrate that this surge can even exceed previous high endemic peaks, unleashing a "grand" pandemic wave after a deceptive calm (Figure 11). This negates all previous efforts and sacrifices, thereby leading to immense socioeconomic impacts. Post-holiday or large-celebration rebound waves in various countries exemplify how uncontrolled mobility and interaction, causing λ shifts, can trigger such disasters.

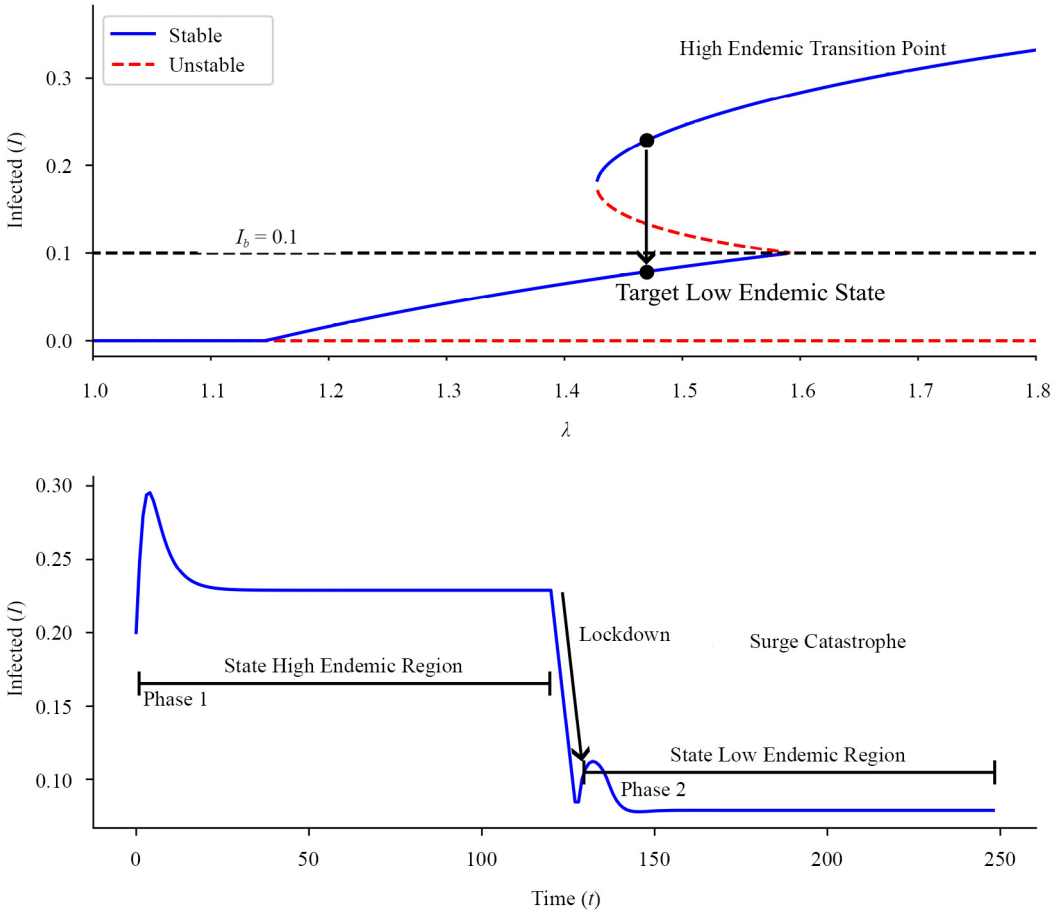

Figure 11. Explosive wave: consequence of a critical shift in λ

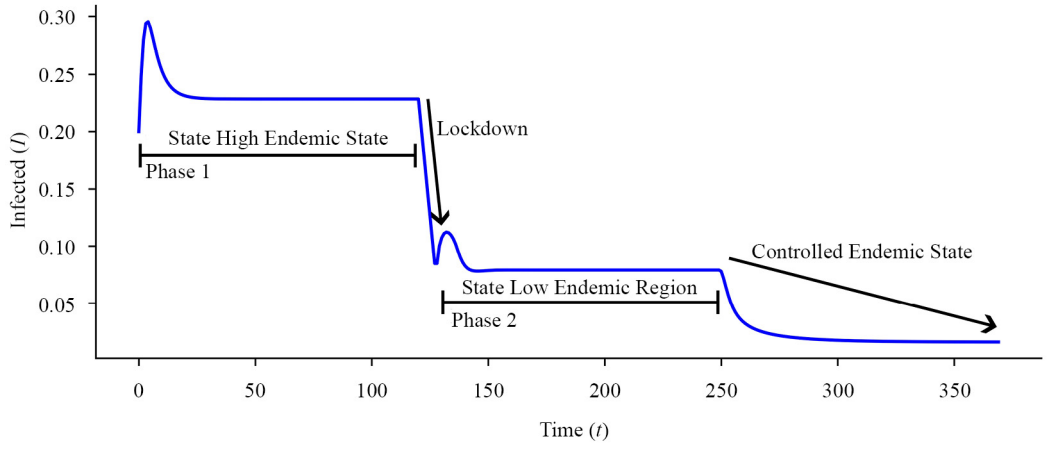

Figure 12. Toward a controlled endemic state: successfully exiting the hysteresis zone

However, if authorities and the public sustain aggressive interventions and push λ left past the λ_{left} threshold, thereby moving out of the hysteresis zone toward a state where only a low endemic (or even DFE) is stable, or toward a controlled

endemic state (a stable condition under which the disease persists at a low and manageable level after successfully exiting the hysteresis zone, differing from a disease-free state), the struggle will yield significant results, as shown in Figure 12. The simulation results confirm that prolonged efforts can push the system left from a high endemic state beyond the hysteresis zone.

However, it is important to note that this outcome may not immediately lead to a DFE. In other words, the system could remain in a stable low endemic state, meaning the disease persists. Even after escaping the hysteresis trap, sustained, long-term efforts, e.g., consistent vaccination strategies, genomic surveillance, and adaptive responses to new variants, are required to continue suppressing λ until DFE is achieved and the disease is eliminated.

4. Conclusion

This study reveals two "pandemic ironies" critical for policymaking, stemming from a dual threshold bifurcation analysis. This analysis establishes a rigorous foundation by formally characterizing the novel Dual Threshold Bifurcation and proving the mathematical existence of the Hysteresis Zone, which governs the system's long-term trajectory. The first underscores the critical need for early intervention. In a pandemic's initial phase, a narrow window of opportunity exists. Bold and immediate action can lead to disease elimination, but hesitation initiates a "Life's Gamble", pushing the system into an endemic trap with massive socioeconomic costs. This entry into the trap occurs when the system crosses the left-side bifurcation threshold, after which return becomes increasingly difficult. The second irony highlights the risks once trapped in this endemic state. In this state, the goal shifts from elimination to mitigation. However, this state is perilous; halfhearted efforts trigger a "rebound trap", and even apparent success creates a "false comfort zone", where the system remains vulnerable to explosive waves from new variants or premature policy easing. This fragility imposes a sustained "cost of remaining", marked by entrenched high public health expenditures that persist even under apparent stability.

The core implication for public health policy is the need for dynamic, threshold-aware strategies. Rather than simple on-off interventions, policies must be designed to consistently push the transmission rate out of the dangerous hysteresis zone. Escaping this trap requires two complementary strategies that act through distinct model mechanisms. First, structural interventions such as vaccination must be sustained to preserve a low endemic equilibrium. Although vaccination does not directly reduce transmission, widespread and continuous immunization enhances system stability and mitigates the risk of sudden rebounds. Second, effective management of initial conditions through aggressive quarantine and isolation is essential to steer the system toward disease elimination, even when circumstances make recovery difficult. Only by doing so can a truly controlled endemic state be achieved, preventing catastrophic surges and minimizing long-term societal harm.

Although the proposed model simplifies real-world complexities—such as assuming stable parameters and a sharp medical capacity threshold—its primary contribution lies in the conceptual framework it provides. Future research can incorporate stochasticity and soft thresholds to capture more nuanced dynamics. Nonetheless, this study provides a dual threshold bifurcation framework that bridges the gap between mathematical epidemiology and practical pandemic policy, offering crucial insights into the early-warning signs that distinguish between a path toward elimination and a fall into an endemic trap. Ultimately, the identification and analytical foundation of the Dual Threshold Bifurcation offer a framework for distinguishing between genuine disease suppression and the illusion of "False Comfort".

Conflict of interest

The authors declare no competing financial interest.

References

[1] Chen Q, Teng Z, Wang F. Fold-flip and strong resonance bifurcations of a discrete-time mosquito model. *Chaos, Solitons and Fractals*. 2021; 144: 110704. Available from: https://doi.org/10.1016/j.chaos.2021.110704.

[2] Al-Basyouni KS, Khan AQ. Discrete-time COVID-19 epidemic model with chaos, stability and bifurcation. *Results in Physics*. 2022; 43: 106038. Available from: https://doi.org/10.1016/j.rinp.2022.106038.

[3] Bucyibaruta G, Dean CB, Torabi M. A discrete-time susceptible-infectious-recovered-susceptible model for the analysis of influenza data. *Infectious Disease Modelling*. 2023; 8(2): 471-483. Available from: https://doi.org/10.1016/j.idm.2023.04.008.

[4] Szabadváry JH, Zhou Y. On qualitative analysis of a discrete time SIR epidemical model. *Chaos, Solitons and Fractals: X*. 2021; 7: 100067. Available from: https://doi.org/10.1016/j.csfx.2021.100067.

[5] Khan AQ. Bifurcations of a two-dimensional discrete-time predator-prey model. *Advances in Difference Equations*. 2019; 2019(1): 56. Available from: https://doi.org/10.1186/s13662-019-1995-6.

[6] Khan AQ, Qureshi SM, Alotaibi AM. Bifurcation analysis of a three species discrete-time predator-prey model. *Alexandria Engineering Journal*. 2022; 61(10): 7853-7875. Available from: https://doi.org/10.1016/j.aej.2021.12.068.

[7] Zhao M. Bifurcation and chaotic behavior in the discrete BVP oscillator. *International Journal of Non-Linear Mechanics*. 2021; 131: 103687. Available from: https://doi.org/10.1016/j.ijnonlinmec.2021.103687.

[8] Huang YJ, Juang J, Kuo TY, Liang YH. Forward-backward and period doubling bifurcations in a discrete epidemic model with vaccination and limited medical resources. *Journal of Mathematical Biology*. 2023; 86(5): 77. Available from: https://doi.org/10.1007/s00285-023-01911-x.

[9] Monteiro LHA. A discrete-time dynamical system with four types of codimension-one bifurcations. *Applied Mathematics and Computation*. 2019; 354: 189-191. Available from: https://doi.org/10.1016/j.amc.2019.02.034.

[10] Gong Y, Small M. Modelling the effect of heterogeneous vaccination on metapopulation epidemic dynamics. *Physics Letters A*. 2019; 383(35): 125996. Available from: https://doi.org/10.1016/j.physleta.2019.125996.

[11] Li Q, Tang B, Bragazzi NL, Xiao Y, Wu J. Modeling the impact of mass influenza vaccination and public health interventions on COVID-19 epidemics with limited detection capability. *Mathematical Biosciences*. 2020; 325: 108378. Available from: https://doi.org/10.1016/j.mbs.2020.108378.

[12] Parolini N, Dede' L, Ardenghi G, Quarteroni A. Modelling the COVID-19 epidemic and the vaccination campaign in Italy by the SUIHTER model. *Infectious Disease Modelling*. 2022; 7(2): 45-63. Available from: https://doi.org/10.1016/j.idm.2022.03.002.

[13] Yang B, Yu Z, Cai Y. The impact of vaccination on the spread of COVID-19: Studying by a mathematical model. *Physica A: Statistical Mechanics and Its Applications*. 2022; 590: 126717. Available from: https://doi.org/10.1016/j.physa.2021.126717.

[14] Kemp F, Proverbio D, Aalto A, Mombaerts L, d'Hérouël AF, Husch A, et al. Modelling COVID-19 dynamics and potential for herd immunity by vaccination in Austria, Luxembourg and Sweden. *Journal of Theoretical Biology*. 2021; 530: 110874. Available from: https://doi.org/10.1016/j.jtbi.2021.110874.

[15] Moh H, Fahreza FR. Herd immunity in a coronavirus disease 2019 epidemic model with consideration of vaccination and quarantine interventions. *Advances in Differential Equations and Control Processes*. 2025; 32(1): 2759. Available from: https://doi.org/10.59400/adecp2759.

[16] Gutiérrez-Jara JP, Vogt-Geisse K, Cabrera M, Córdova-Lepe F, Muñoz-Quezada MT. Effects of human mobility and behavior on disease transmission in a COVID-19 mathematical model. *Scientific Reports*. 2022; 12(1): 10840. Available from: https://doi.org/10.1038/s41598-022-14155-4.

[17] Chen S, Janies D, Paul R, Thill JC. Leveraging advances in data-driven deep learning methods for hybrid epidemic modeling. *Epidemics*. 2024; 48: 100782. Available from: https://doi.org/10.1016/j.epidem.2024.100782.

[18] Demongeot J, Magal P. Data-driven mathematical modeling approaches for COVID-19: A survey. *Physics of Life Reviews*. 2024; 50: 166-208. Available from: https://doi.org/10.1016/j.plrev.2024.08.004.

[19] Ferreira LS, Canton O, da Silva RLP, Poloni S, Sudbrack V, Borges ME, et al. Assessing the best time interval between doses in a two-dose vaccination regimen to reduce the number of deaths in an ongoing epidemic of SARS-CoV-2. *PLOS Computational Biology*. 2022; 18(3): e1009978. Available from: https://doi.org/10.1371/journal.pcbi.1009978.

[20] Islas JM, Corona-Moreno R, Velasco-Hernández JX. Multiple endemic equilibria in an environmentally-transmitted disease with three disease stages. *Mathematical Biosciences*. 2024; 375: 109244. Available from: https://doi.org/10.1101/2024.03.21.24304681.

[21] Owen L, Hoseana J, Yong B. A numerical study of codimension-two bifurcations of an SIR-type model for COVID-19 and their epidemiological implications. *Communication in Biomathematical Sciences*. 2023; 6(2): 156-168. Available from: https://doi.org/10.5614/cbms.2023.6.2.6.

[22] Nisar KS, Farman M, Abdel-Aty M, Cao J. A review on epidemic models in sight of fractional calculus. *Alexandria Engineering Journal*. 2023; 75: 81-113. Available from: https://doi.org/10.1016/j.aej.2023.05.071.

[23] Riaz M, Khan ZA, Ahmad S, Ateya AA. Fractional-order dynamics in epidemic disease modeling with advanced perspectives of fractional Calculus. *Fractal and Fractional*. 2024; 8(5): 291. Available from: https://doi.org/10.3390/fractalfract8050291.

[24] Fahreza FR, Hasan M, Santoso KA. Chaotic outbreak in discrete epidemic model with vaccination and quarantine interventions and limited medical resources. *Scientific Journal of Mathematics and Statistics*. 2025; 25(1): 22-35. Available from: https://doi.org/https://doi.org/10.19184/mims.v25i1.53689.

[25] Angeli F, Montefusco A. Sensemaking and learning during the Covid-19 pandemic: A complex adaptive systems perspective on policy decision-making. *World Development*. 2020; 136: 105106. Available from: https://doi.org/10.1016/j.worlddev.2020.105106.

[26] Chorus C, Sandorf ED, Mouter N. Diabolical dilemmas of COVID-19: An empirical study into Dutch society's trade-offs between health impacts and other effects of the lockdown. *PLOS One*. 2020; 15(9): e0238683. Available from: https://doi.org/10.1371/journal.pone.0238683.

[27] Dobson A, Ricci C, Boucekkine R, Gozzi F, Fabbri G, Loch-Temzelides T, et al. Balancing economic and epidemiological interventions in the early stages of pathogen emergence. *Science Advances*. 2023; 9(21): eade6169. Available from: https://doi.org/10.1126/sciadv.ade6169.

[28] Cross M, Ng SK, Scuffham P. Trading Health for Wealth: The Effect of COVID-19 Response Stringency. *International Journal of Environmental Research and Public Health*. 2020; 17(23): 8725. Available from: https://doi.org/10.3390/ijerph17238725.

[29] Allen LJS. *An Introduction to Mathematical Biology*. New York: Pearson/Prentice Hall; 2007.

[30] Cushing JM. *Matrix Models for Population, Disease, and Evolutionary Dynamics*. Vol. 106. Rhode Island: American Mathematical Society; 2024.

[31] Keyfitz N, Caswell H. *Applied Mathematical Demography*. 3rd ed. New York: Springer Verlag; 2005.

[32] Dickson LE. *First Course in the Theory of Equations*. New York: John Wiley and Sons, Inc; 2009.

[33] Smith B. First covid lockdown was delayed because 'There was no plan', cummings says. *Civil Service World*. 2021. Available from: https://www.civilserviceworld.com/news/article/first-covid-lockdown-was-delayed-because-there-was-no-plan-cummings-says.

[34] Ahlander J, Pollard N. Sweden acted too slowly as pandemic swept country, commission finds. *Reuters*. 2021. Available from: https://www.reuters.com/world/sweden-acted-too-slowly-pandemic-hit-commission-finds-2021-10-29/.

[35] Mao Y, Wang W, Ma J, Wu S, Sun F. Reinfection rates among patients previously infected by SARS-CoV-2: systematic review and meta-analysis. *Chinese Medical Journal*. 2022; 135(2): 145-152. Available from: https://doi.org/10.1097/CM9.0000000000001892.

[36] Roache M. Europe's second wave of COVID-19 is being driven by two countries. Here's why. *TIME*. 2020. Available from: https://time.com/5902172/europe-coronavirus-second-wave-belgium-czech-republic/.

[37] Mackintosh E. Masks are back, as delta variant forces dramatic reversal in US. *CNN*. 2021. Available from: https://edition.cnn.com/2021/07/28/world/coronavirus-newsletter-intl-28-07-21.

[38] Worldometer. Indonesia COVID-coronavirus statistics. *Worldometer*. 2024. Available from: https://www.worldometers.info/coronavirus/country/indonesia/.

[39] Pasricha A. India opens up, but threat of a third COVID wave looms. *VOA News*. 2021. Available from: https://www.voanews.com/a/covid-19-pandemic_india-opens-threat-third-covid-wave-looms/6209567.html.

Appendix A. Proof of positivity and boundedness

A.1 *Positivity of solutions*

For the model in System (1) to be epidemiologically meaningful, each state variable must remain non-negative at all time steps. In other words, the number of individuals in each compartment should never be negative. The intuition behind this proof is simple: in one time step, the total probability of an individual moving out of a compartment cannot exceed one. Assuming the time step length used is $\Delta t = 1$, this can be achieved by ensuring that the parameters and variable values at time t are chosen such that the total outflow rate from each compartment is always between zero and one.

For example, consider the susceptible population compartment, S_t, which follows the equation:

$$S_{t+1} = S_t - (\lambda I_t + \lambda q Q_t + \varphi_1 + \mu) S_t + \Lambda + \rho R_t.$$

Here, the total outflow rate from compartment S_t can be defined as $k_{out,S} = (\lambda I_t + \lambda q Q_t + \varphi_1 + \mu)$. Assuming $0 \leq k_{out,S} \leq 1$, the probability of someone remaining in the susceptible compartment, i.e., $(1 - k_{out,S})$, will always be non-negative. If the initial population is in a non-negative condition, i.e., $S_0 \geq 0$, then using induction, it can be shown that S_t will remain non-negative for all t. Assuming $S_t \geq 0$, the above equation can be rewritten as:

$$S_{t+1} = S_t(1 - k_{out,S}) + (\Lambda + \rho R_t).$$

Since $(1 - k_{out,S}) \geq 0$, $S_t \geq 0$, and the inflow terms like Λ and ρR_t are also non-negative by definition, every term on the right-hand side of this equation must be non-negative. Therefore, S_{t+1} is also guaranteed to be non-negative.

The same logic can be applied to all other compartments in the model. For example, for the population receiving the first dose of the vaccine, V_{1_t}, the required condition is $(\lambda p I_t + \lambda p q Q_t + \varphi_2 + \mu) \leq 1$. As long as the total outflow rate from each compartment satisfies this fundamental condition, all state variables in the system will remain non-negative for all times $t \geq 0$. This ensures that the model does not produce unrealistic population values, such as negative numbers of individuals, and remains consistent with correct epidemiological interpretations.

A.2 *Boundedness of solutions*

To show that the model solution remains bounded, we begin by analyzing the total population living in the system, denoted by N_t. The death compartment D_t is excluded because it represents individuals who have left the living population. Total population is defined as:

$$N_t = S_t + V_{1_t} + V_{2_t} + I_t + Q_t + R_t.$$

By summing the first six equations from System (1), we obtain an equation for N_{t+1} that describes the population change from one time step to the next. In this addition process, all terms that only move individuals between compartments cancel each other out. This includes transmission due to infection, vaccination, quarantine, recovery, and reinfection. All that remains are the terms representing the inflow into the system (births or immigration, Λ) and the outflow from the system (natural deaths, μ, as well as deaths due to disease, ζ).

The final result can be written as:

$$N_{t+1} = N_t + \Lambda - \mu N_t - (\zeta I_t + \zeta d Q_t).$$

Since the number of deaths from a disease is always non-negative, we can form the inequality:

$$N_{t+1} \leq (1-\mu)N_t + \Lambda.$$

This inequality shows that the total population N_t is limited. Specifically, if N_t exceeds $\frac{\Lambda}{\mu}$, the value of N_t in the next step will not increase further, but will tend to decrease. In other words, $\frac{\Lambda}{\mu}$ acts as an upper bound for the population. Therefore, in the long run, the total population will always be below or equal to this value:

$$\limsup_{t\to\infty} N_t \leq \frac{\Lambda}{\mu}.$$

Since it has been previously proven that each compartment is non-negative, and now the total population N_t is proven to be limited, it logically follows that each individual compartment ($S_t, V_{1_t}, \ldots, R_t$) must also be limited. Thus, this model is guaranteed to have a well-defined solution and be within a biologically feasible range. Note that the closed-system assumption ($\Lambda = \mu N$) used in our equilibrium analysis is a specific case of this general boundedness, ensuring that the disease-free population stabilizes at the upper bound $N = \frac{\Lambda}{\mu}$.

Appendix B. Proof of local asymptotic stability of the DFE (Ω_0)

To determine whether the DFE, denoted by Ω_0, is stable, we examine the eigenvalues of the Jacobian matrix, $\mathbf{J}(\Omega_0)$, evaluated at this point. In a discrete-time system, the DFE is said to be locally asymptotically stable if all eigenvalues (β_i) satisfy the condition $|\beta_i| < 1$. This means that any small perturbation from the DFE will disappear over time and the system will return to a disease-free state.

The Jacobian matrix at the DFE has a block form:

$$\mathbf{J}(\Omega_0) = \begin{bmatrix} \mathbf{J}_{11} & \mathbf{J}_{12} \\ \\ \mathbf{0} & \mathbf{J}_{22} \end{bmatrix},$$

where $\mathbf{J}_{11}$ is related to the uninfected compartments (S, V_1, V_2, R), while $\mathbf{J}_{22}$ is related to the infected compartments (I, Q). Due to this block form, the eigenvalues of $\mathbf{J}(\Omega_0)$ are sufficiently determined by the eigenvalues of each block, namely $\mathbf{J}_{11}$ and $\mathbf{J}_{22}$.

For $\mathbf{J}_{11}$, the eigenvalues can be directly obtained from the diagonal elements:

$$\beta_1 = 1-(\mu+\varphi_1), \quad \beta_2 = 1-(\mu+\varphi_2), \quad \beta_3 = 1-\mu, \quad \beta_4 = 1-(\rho+\mu).$$

Since all parameters μ, φ_1, φ_2, and ρ are positive and less than 1, these four values automatically satisfy $|\beta_i| < 1$. In other words, the uninfected compartment does not affect stability. Therefore, the overall stability of the DFE is determined entirely by the infected compartment, i.e., $\mathbf{J}_{22}$.

The submatrix $\mathbf{J}_{22}$ can be written as:

$$\mathbf{J}_{22} = \begin{bmatrix} a_{11} & a_{12} \\ \\ a_{21} & a_{22} \end{bmatrix} = \begin{bmatrix} 1-k_3+\mathscr{A} & q\mathscr{A}+\tau_2 \\ \\ \tau_1 & 1-k_4 \end{bmatrix},$$

where $\mathscr{A} = \frac{\Lambda\lambda((p\varphi_1+k_2)\mu+\varphi_1\varphi_2 r)}{\mu k_1 k_2}$, while k_3 and k_4 are combined parameters defined in the main text.

The eigenvalues of this matrix are determined by the characteristic equation:

$$\beta^2 - \mathrm{Tr}(\mathbf{J}_{22})\,\beta + \det(\mathbf{J}_{22}) = 0,$$

with $\mathrm{Tr}(\mathbf{J}_{22})$ as the trace (sum of diagonal elements) and $\det(\mathbf{J}_{22})$ as the determinant.

For a second-order discrete system, Jury's criterion states that the DFE is stable if and only if the following three conditions are met:

1. $1-\mathrm{Tr}(\mathbf{J}_{22})+\det(\mathbf{J}_{22}) > 0$,
2. $1+\mathrm{Tr}(\mathbf{J}_{22})+\det(\mathbf{J}_{22}) > 0$,
3. $|\det(\mathbf{J}_{22})| < 1$.

In discrete epidemiological theory, it is known that these three conditions can be combined and written in a simpler form: DFE is stable if and only if the basic reproduction number, $\mathscr{R}_0$, is less than one.

Let's look at the first condition, which is usually the most important. If we calculate it directly, we get

$$1 - \mathrm{Tr}(\mathbf{J}_{22}) + \det(\mathbf{J}_{22}) = (k_3k_4 - \tau_1\tau_2) - \mathscr{A}(q\tau_1 + k_4).$$

Since $(k_3k_4 - \tau_1\tau_2) > 0$ for biologically feasible models, we can divide both sides by this term and obtain

$$1 - \frac{\mathscr{A}(q\tau_1 + k_4)}{k_3k_4 - \tau_1\tau_2} > 0.$$

The above definition aligns with the definition of the basic reproduction number, which is

$$\mathscr{R}_0 = \frac{\mathscr{A}(q\tau_1 + k_4)}{k_3k_4 - \tau_1\tau_2}.$$

Thus, the stability condition can be simplified to

$$1 - \mathscr{R}_0 > 0 \quad \Rightarrow \quad \mathscr{R}_0 < 1.$$

Similarly, the other two Jury conditions can also be proven true, assuming all model parameters are positive and epidemiologically plausible. For example, the determinant can be rewritten as

$$\det(\mathbf{J}_{22}) = (1 - k_3)(1 - k_4) + \mathscr{A}(1 - k_4) - \tau_1(q\mathscr{A} + \tau_2),$$

which satisfies $|\det(\mathbf{J}_{22})| < 1$ if $\mathscr{R}_0 < 1$.

From the discussion above, it can be concluded that the DFE is locally asymptotically stable if and only if $\mathscr{R}_0 < 1$. If $\mathscr{R}_0$ exceeds 1, the DFE point becomes unstable and the disease will spread in the population. This proves a direct relationship between the basic reproduction number and the stability of the modeled epidemiological system.

Appendix C. Components of the endemic equilibrium Ω_1 ($I^* \leq I_b$)

$$S_1 = \frac{\Lambda+\rho R_1}{\alpha+k_1}, \qquad V_{1_1} = \frac{\varphi_1 S_1}{\alpha p+k_2}, \qquad V_{2_1} = \frac{\varphi_2 V_{1_1}}{\alpha r+\mu},$$

$$\begin{aligned} I_1 = -[&\alpha(p\alpha^2 r + (p\mu + r(p\varphi_1 + k_2))\alpha + (p\varphi_1 + k_2)\mu + \varphi_1\varphi_2 r)k_4(\rho+\mu)\Lambda]/[pr(((\gamma_n + \gamma_m - k_3)k_4 + \tau_1(\tau_2 + \\ &\gamma_n))\rho + \mu(-k_3k_4 + \tau_1\tau_2))\alpha^3 + ((p((\gamma_n+\gamma_m-k_3)k_4 + \tau_1(\tau_2+\gamma_n))\mu + (((-k_3k_1 + \varphi_1(\gamma_n+\gamma_m))k_4 + \tau_1(\gamma_n\varphi_1 + \\ &k_1\tau_2))p + ((\gamma_n+\gamma_m-k_3)k_4 + \tau_1(\tau_2+\gamma_n))k_2)r)\rho + (p\mu + r(k_1p+k_2))(-k_3k_4 + \tau_1\tau_2)\mu)\alpha^2 + (((((-k_3k_1 + \\ &\varphi_1(\gamma_n+\gamma_m))k_4 + \tau_1(\gamma_n\varphi_1 + k_1\tau_2))p + ((\gamma_n+\gamma_m-k_3)k_4 + \tau_1(\tau_2+\gamma_n))k_2)\mu + r((-k_3k_1k_2 + \varphi_1\varphi_2(\gamma_n+\gamma_m))k_4 + \\ &\tau_1(\gamma_n\varphi_1\varphi_2 + k_1k_2\tau_2)))\rho + ((k_1p+k_2)\mu + rk_1k_2)(-k_3k_4 + \tau_1\tau_2)\mu)\alpha + k_1k_2\mu(\rho+\mu)(-k_3k_4 + \tau_1\tau_2)], \end{aligned}$$

$$Q_1 = \frac{\tau_1 I_1}{k_4}, \qquad R_1 = \frac{I_1\gamma_n + I_1\gamma_m + \gamma_n Q_1}{\rho+\mu}.$$

Appendix D. Coefficients of equation (3)

$$A = -p(\mu^3 + ((d+1)\zeta + \gamma_m + \rho + \tau_1 + \tau_2 + 2\gamma_n)\mu^2 + (d\zeta^2 + ((d+1)\rho + (d+1)\gamma_n + (\gamma_m + \tau_1)d + \tau_2)\zeta + (\tau_1 + \tau_2 + \gamma_n)\rho + \gamma_n^2 + (\gamma_m + \tau_1 + \tau_2)\gamma_n + \gamma_m\tau_2)\mu + \rho\zeta(d\tau_1 + \zeta d + \gamma_n + \tau_2))r,$$

$$B = ((((\lambda\Lambda + \gamma_n\varphi_1 + \varphi_1\gamma_m - k_3k_1)k_4 + \tau_1(\Lambda\lambda q + \gamma_n\varphi_1 + k_1\tau_2))\rho + ((\lambda\Lambda - k_3k_1)k_4 + \tau_1(\Lambda\lambda q + k_1\tau_2))\mu)r + (((\gamma_n + \gamma_m - k_3)k_4 + \tau_1(\tau_2 + \gamma_n))\rho + \mu(-k_3k_4 + \tau_1\tau_2))\mu)p + r(((\gamma_n + \gamma_m - k_3)k_4 + \tau_1(\tau_2 + \gamma_n))\rho + \mu(-k_3k_4 + \tau_1\tau_2))k_2,$$

$$C = (((\lambda\Lambda - k_3k_1)p - k_2k_3)k_4 + \tau_1((\Lambda\lambda q + k_1\tau_2)p + \tau_2k_2))\mu^2 + ((((-k_3k_1 + \varphi_1(\gamma_n + \gamma_m) + \lambda\Lambda)p + k_2(\gamma_n + \gamma_m - k_3))k_4 + \tau_1((\Lambda\lambda q + \gamma_n\varphi_1 + k_1\tau_2)p + k_2(\tau_2 + \gamma_n)))\rho + r((p\Lambda\lambda\varphi_1 + (\lambda\Lambda - k_3k_1)k_2)k_4 + \tau_1(p\Lambda\lambda\varphi_1 q + (\Lambda\lambda q + k_1\tau_2)k_2)))\mu + r\rho(((\lambda\Lambda - k_3k_1)k_2 + (p\Lambda\lambda + \varphi_2(\gamma_n + \gamma_m))\varphi_1)k_4 + \tau_1((\Lambda\lambda q + k_1\tau_2)k_2 + \varphi_1(\Lambda\lambda pq + \gamma_n\varphi_2))),$$

$$E = -k_1(\mu^2 + ((d+1)\zeta + \gamma_m + \tau_1 + \tau_2 + 2\gamma_n)\mu + d\zeta^2 + ((d+1)\gamma_n + (\gamma_m + \tau_1)d + \tau_2)\zeta + \gamma_n^2 + (\gamma_m + \tau_1 + \tau_2)\gamma_n + \gamma_m\tau_2)k_2(\rho + \mu)\mu.$$

Appendix E. Components of the endemic equilibrium Ω_2 ($I^* > I_b$)

$$S_2 = \frac{((I_b\gamma_m + I_2\gamma_n + \Lambda)\rho + \mu\Lambda)k_4 + I_2\gamma_n\rho\tau_1}{(\rho+\mu)((\lambda I_2 + k_1)k_4 + \tau_1 I_2\lambda q)},$$

$$V_{1_2} = \frac{k_4((\gamma_n I_2\rho + (I_b\gamma_m + \Lambda)\rho + \mu\Lambda)k_4 + I_2\gamma_n\rho\tau_1)\varphi_1}{((\lambda I_2 + k_1)k_4 + \tau_1 I_2\lambda q)(\rho+\mu)((I_2\lambda p + k_2)k_4 + I_2\lambda pq\tau_1)},$$

$$V_{2_2} = \frac{((\gamma_n I_2\rho + (I_b\gamma_m + \Lambda)\rho + \mu\Lambda)k_4 + I_2\gamma_n\rho\tau_1)k_4^2\varphi_2\varphi_1}{((I_2\lambda r + \mu)k_4 + \tau_1 I_2\lambda qr)((\lambda I_2 + k_1)k_4 + \tau_1 I_2\lambda q)(\rho+\mu)((I_2\lambda p + k_2)k_4 + I_2\lambda pq\tau_1)},$$

$$Q_2 = \frac{\tau_1 I_2}{k_4},$$

$$R_2 = \frac{I_2(k_4 + \tau_1)\gamma_n + I_b\gamma_m k_4}{k_4(\rho+\mu)}.$$

Appendix F. Parameters of the quartic equation (5)

$$A_2 = -p(q\tau_1 + k_4)^3 r(((-\gamma_n - \tau_2)\rho - \mu\tau_2)\tau_1 + k_4(\rho k_5 + \mu(\gamma_n + k_5))),$$

$$B_2 = -pr(q\tau_1 + k_4)((-\mu - \rho)\Omega + \gamma_m I_b \mu),$$

$$B_3 = ((k_1((-\gamma_n - k_5)k_4 + \tau_1\tau_2)\mu + (((\varphi_1 - k_1)\gamma_n - k_1 k_5)k_4 + \tau_1(\gamma_n\varphi_1 + k_1\tau_2))\rho)r + (((-\gamma_n - k_5)k_4 + \tau_1\tau_2)\mu + \rho(-k_4k_5 + \tau_1(\tau_2 + \gamma_n)))\mu)p + (((-\gamma_n - k_5)k_4 + \tau_1\tau_2)\mu + \rho(-k_4k_5 + \tau_1(\tau_2 + \gamma_n)))k_2 r,$$

$$C_2 = (q\tau_1 + k_4)(((((-\gamma_m I_b k_1 + \Omega\varphi_1)\mu + (I_b(\varphi_1 - k_1)\gamma_m + \Omega\varphi_1)\rho)r + \mu((-I_b\gamma_m + \Omega)\mu + \rho\Omega))p + k_2((-I_b\gamma_m + \Omega)\mu + \rho\Omega)r),$$

$$C_3 = (k_1 p + k_2)((-\gamma_n - k_5)k_4 + \tau_1\tau_2)\mu^2 + (((-k_1(\gamma_n + k_5)p + p\gamma_n\varphi_1 - k_2k_5)k_4 + \tau_1(k_1\tau_2 p + k_2(\tau_2 + \gamma_n) + p\gamma_n\varphi_1))\rho + k_2 r k_1((-\gamma_n - k_5)k_4 + \tau_1\tau_2))\mu + \rho r((-k_1(\gamma_n + k_5)k_2 + \gamma_n\varphi_1\varphi_2)k_4 + (\gamma_n\varphi_1\varphi_2 + k_1k_2\tau_2)\tau_1),$$

$$E_2 = (q\tau_1 + k_4)((-I_b(k_1 p + k_2)\gamma_m + \Omega(p\varphi_1 + k_2))\mu^2 + ((p(\varphi_1 - k_1)\rho - k_2 r k_1)I_b\gamma_m + \Omega((p\varphi_1 + k_2)\rho + \varphi_1\varphi_2 r))\mu + (I_b(-k_1k_2 + \varphi_1\varphi_2)\gamma_m + \Omega\varphi_1\varphi_2)\rho r),$$

$$E_3 = -(\rho + \mu)k_1((\gamma_n + k_5)k_4 - \tau_1\tau_2)k_2\mu,$$

$$F_1 = -\mu\gamma_m I_b k_1 k_2 k_4^4(\rho + \mu),$$

$$k_5 = \tau_1 + \mu + \zeta.$$